Ca' Foscari
University
of Venice

Master's Degree Programme in Sustainable Chemistry and Technologies

Second Cycle
(D.M.270/2004)

Final Thesis

Development of heterogeneous catalysts for levulinic acid production

Supervisor
Prof. Michela Signoretto

Assistant supervisor
Dr. Federica Menegazzo

Graduand
Gea Bortolomiol
Matriculation Number 844003

Academic Year
2017 / 2018

“Ἐν πᾶσι γὰρ τοῖς φυσικοῖς ἔνεστί τι θαυμαστόν”

“In all natural things there is something marvelous”

Aristotele, 384-322 B.C.

Contents

1. INTRODUCTION 2
   1.1 Sustainability and renewables 2
   1.1.1 Biomass as a renewable resource 3
   1.1.2 From biomass to chemicals 5
   1.1.3 Lignocellulosic biomass 6
   1.2 Levulinic acid production 8
   1.3 Ordered Mesoporous Silica catalysts 15
   1.3.1 SBA-15 and its possible modifications 17
2. AIM OF THE WORK 20
3. MATERIALS AND METHODS 21
   3.1 Synthesis 21
   3.1.1 Synthesis of SBA-15 21
   3.1.2 Synthesis using the Ti salt 22
   3.1.3 Synthesis using Acetylacetone as chelating agent 23
   3.1.4 MPTMS grafting and oxidation 24
   3.2 Characterizations 25
   3.2.1 Nitrogen Physisorption 25
   3.2.2 X-Ray Diffraction (XRD) 27
   3.2.3 Temperature Programmed Oxidation (TPO) 29
   3.2.4 Titration method 30
   3.3 Tests 31
   3.3.1 Mechanical stability tests 31
   3.3.2 Hydrothermal stability tests 31
   3.3.3 Reactivity tests 31
4. RESULTS AND DISCUSSION 33
5. CONCLUSION 47
6. APPENDIX 48
7. REFERENCES 52

1. INTRODUCTION

1.1 Sustainability and renewables

One of the major issue of our modern society is to guide future development to a progressive replacement of fossil resources. These indeed still provide more than 80% of our energy needs and 95% of the chemical feedstocks. Depletion of nonrenewable sources, together with the increasing energy demand, has brought several economic, political and environmental concerns.

Due to a rising global population, world's overall energy demand is expected to rise 2% per annum, resulting the 2050 energy consumption predicted to be twice that of 2001.[1] Besides, the increased need of energy and resources is strictly related to global warming threat, as carbon dioxide emissions are increasing and they reached the value of 33.4 GT in 2016.[2]

The economic aspect connected to the use of carbon fossil fuels as primary resources is also crucial. In fact, in the last decades, the cost of crude oil has been unstable and markedly affected by strategic decisions of the major political realities and even if weakly, its actual economical trend is rising.[3]

All these aspects have addressed worldwide governments to promote research and investments from fossil fuels to renewable alternatives, in combination with the reduction of CO_2 emissions. The increased interest over sustainable development's issues was signed by different political maneuverings like the Kyoto protocol (2005), the Copenhagen Accord (2009) and the Paris COP 21 UN conference (2015) which heralded what some considered the dawn of the postfossil fuel era.[4-6]

Total renewable energy consumption is expected to increase by almost 30% over 2018-2023, covering more than 40% of global total energy demand growth.[7]

In this scenario biomass resources play an important role.

Particularly bioenergy, namely the energy obtained from biomass – as solid, gaseous or liquid fuels – is expected to be the largest source over renewable consumption in terms of absolute value. *(Figure 1)* This source of energy will be predominantly used for heat and transport, while other renewables have less penetration in these two sectors, which together account for 80% of total energy consumption.[8]

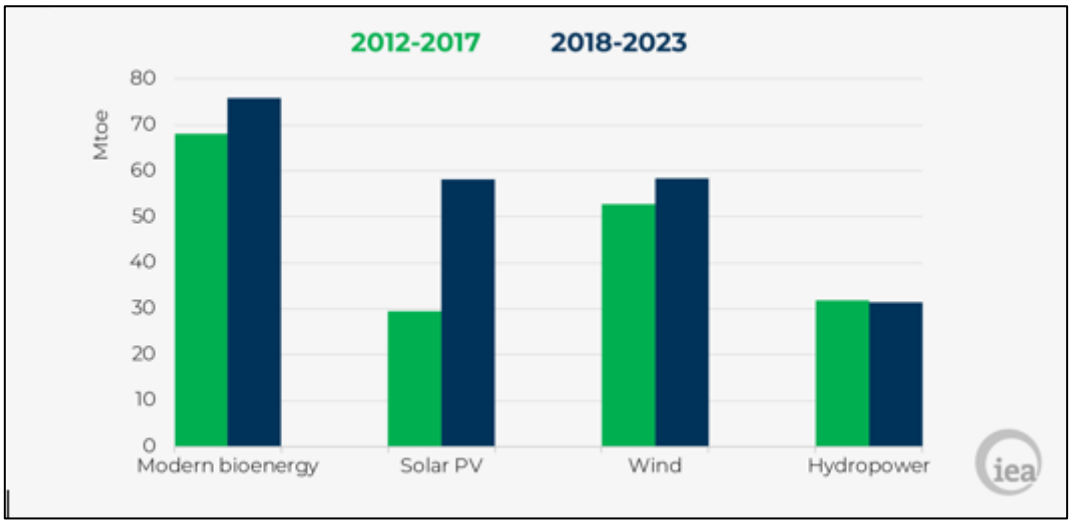

Figure 1: Total energy consumption growth of renewables over 2018-23.[8]

Biomass is one of the most prominent alternatives to fossil carbon resources and its use is strictly related to the modern concept of bioeconomy, which includes the employment of biological renewables in order to convert them into food, bioenergy and bio-based products.[9] Indeed, biomass valorization is one of the strategic topics of Horizon 2020 (H2020), the European Union Framework Programme for Research and Innovation for 2014-2020.[10]

1.1.1 Biomass as a renewable resource

Biomass is the oldest energy source used by mankind and it has been used as source for production of chemicals since ancient times. Nonetheless, its influence over global policy raised after the energy crisis at the end of the 70's, together with the development of economic, social and environmental concerns. According to the directive 2009/28/EC of the European Parliament the term "biomass" refers to "*the biodegradable fraction of products, waste and residues from biological origin from agriculture (including vegetal and animal substances), forestry and related industries including fisheries and aquaculture, as well as the biodegradable fraction of industrial and municipal waste*".[11]

Biomass is a complex matrix whose composition varies due to the origin and nature of the raw material. Unlike crude oil and gas, it is a globally available, natural carbon resource, whose main components are carbohydrates (ca.75%).[12] If a program of replacement is managed, biomass can be considered as a renewable resource, that is available on human timescale.[13] Annually, around 115 x 10^9 tons of atmospheric C are transformed into biomass

through the photosynthesis process[14] and global biomass production assessment amounts to ca. 10^{11} tons.[15] Indeed, biomass can be considered a clean source, as its use takes part in a carbon neutral circular framework, because it neither affects the natural C-CO_2 cycle nor contributes to a built-up of greenhouse gases in the atmosphere.[16] *(Figure 2)*
Therefore, biomass is the most promising renewable source of fixed organic carbon, which is essential for the production of both fuels and chemicals.[17] However, less than 5% of biomass is cultivated, harvested and used, including both food and non-food goals.[18]

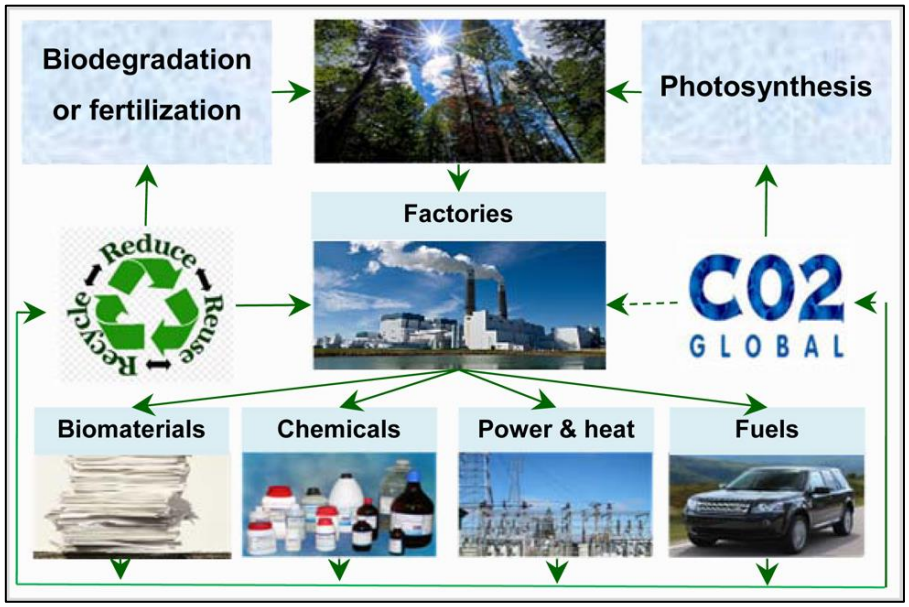

Figure 2: Carbon neutral circular framework of biomass.[16]

Biomass is classified into three classes: the first, the second and the third generation. Since the exploitation of first-generation biomasses, which are used as feedstock by the primary sector, impacts upon food supply and prices, thus generating economic, social and ethical controversies, the importance of the diversification of the biomass' sources has emerged. In this scenario, inedible and waste biomass feedstocks, named lignocellulose biomasses, which are known as second generation ones, play a crucial role. The "zero waste economy concept" has made much effort towards a sustainable development, highlighting the importance of various types of waste (i.e. forest and agricultural waste, municipal waste and manure) as valuable raw materials, thus enshrining the end of edible biomasses utilization as source.[19,20]

The third type of biomasses come from algae and marginal lands cultivations, as well as genetically modified microorganisms and plants employed for precise exploitation purposes.[21]

As current overall trend biomass' demand is increasing worldwide and the EEA (European Environment Agency) estimates that the European production capacity could grow up to 300 Mtons by 2030.[22]

1.1.2 From biomass to chemicals

The facility in which biological raw material are transformed and further converted into energy, heat and value-added chemical commodities is known as biorefinery.[23]

Biorefineries should permit the efficient and flexible use of biomass through the application of innovative and sustainable technologies. In order to have at its disposal feasible and economically competitive biorefineries, a bio-based economy necessarily requires a deep knowledge of the substrate characteristics (i.e. biomass composition and energy content) and the development of appropriate pretreatment and conversion technology processes.[24,25]

Due to its complex structures, efficient conversion of biomass into fuels and valuable chemicals requires at least one pretreatment step, which includes various technologies.[26,27]

Conversion step itself can be done using different kind of strategies, which involve physical, thermal (pyrolysis, gasification, and liquefaction), biological (fermentation and digestion) and chemocatalytic technologies.[28] Other methods for biomass conversion include supercritical approach and hydrothermal upgrading, however these ways are still in a development stage and their use is discouraged by both high costs and harsh conditions required.[29,30]

The future biorefinery will take part of a fully integrated agro-biofuel-biomaterial-biopower cycle, where renewable feedstocks can be incorporated in higher value-added commercial scale processes.[31] In this perspective a major challenge is to convert biomass into chemicals.

From the chemical point of view, biomass differs from fossil feedstocks because it is highly functionalized and has a significantly higher oxygen content that could be up to 40 wt.%.[32]

The overabundance of chemical targets and the contemporary lack of conversion technology motivated the US Department of Energy (DOE) to promote research in biomass valorization. In 2004 DOE published a report combining the identification of 15 organic molecules derived from biorefinery carbohydrates with technology needs for their

production.[33] Those molecules are known as Biobased Chemical Building Blocks (BCBBs) and include furan species, organic acids, polyols and aminoacids.*(Figure 3)*

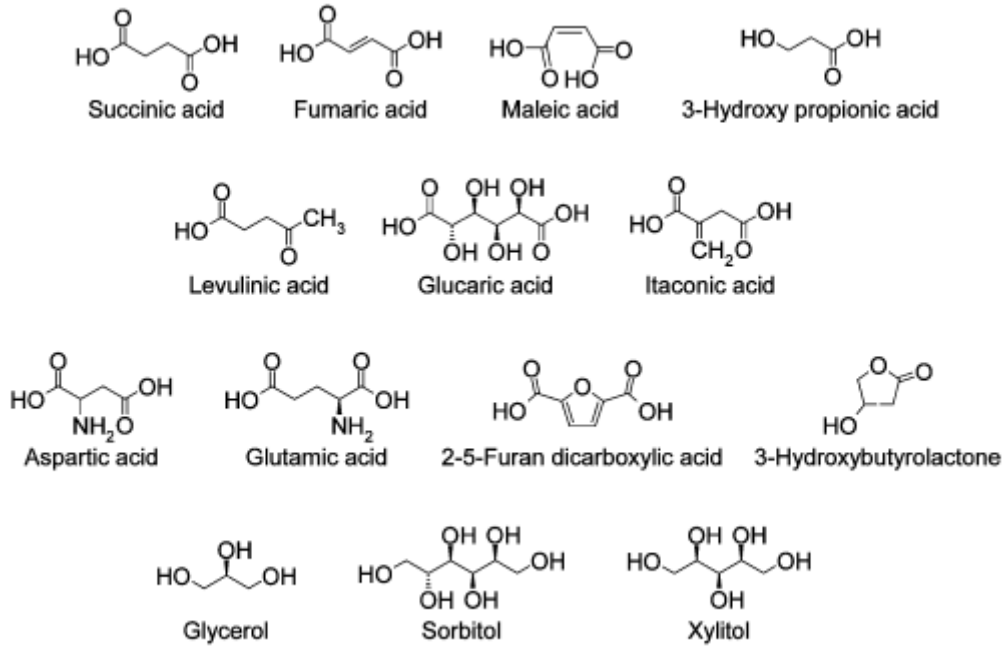

Figure 3: BCBBs identified by DOE in 2004.[16]

BCBBs are target species of strategic importance as they can act as platform chemical for the synthesis of high value-added chemicals and biomaterials.

1.1.3 Lignocellulosic biomass

Lignocellulosic biomass is the most abundant inedible biomass, thus representing a promising source to produce bio-derived chemicals.[34]

Indeed, the past few decades have witnessed considerable attention towards valorization of this kind of natural feedstock.

Lignocellulosic biomass major components are three different oxygen-containing high-molecular-weight polymers. They include cellulose, which is generally the largest fraction of the biomass (40-60 wt.%), hemicellulose (15-30 wt.%) and lignin (10-25 wt.%).[35] The biomass composition depends on its source, for example softwoods contain higher lignin and fewer carbohydrates on average.[36] Other minor constituents of lignocellulosic biomass

are proteins, lipids, as well as resins, tannins, fatty acids, vitamins, dyes, aromatic essence, flavors and inorganic salts.[37]

Cellulose is a water insoluble, linear polysaccharide formed by C_6-glucose units linked by *β*(1-4) glycosidic bonds.[38] Indeed, cellulose is the most abundant biopolymer on earth. Using conversion technologies this polyose can be hydrolyzed into its glucose monomers enabling the synthesis of a large number of chemicals based on the so-called sugar derived platform molecules. [39,40]

Hemicellulose is a heteropolymer which consist of pentose (mainly xylose) and hexose units, connected by different glycosidic bonds.[41]

Together cellulose and hemicellulose are embedded in a lignin matrix.*(Figure 4)*

Lignin is an amorphous polymer made by a three-dimensional network of polyaromatic alcohols. The complex derived structure consists of various methoxylated phenylpropane units which primary derive from *p*-coumaryl, coniferyl and sinapyl alcohols. The functional property of lignin in woody biomass is providing rigidity, strength and resistance to degradation.[42]

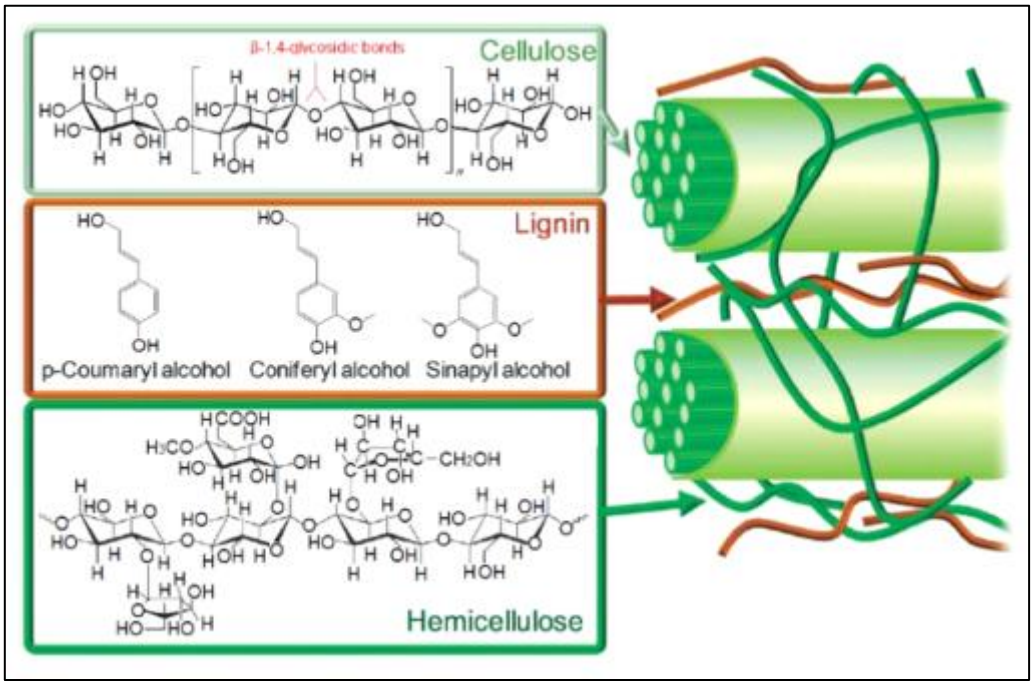

Figure 4: Main components of lignocellulosic biomass.[38]

Both highly functionalized carbohydrates provided by natural cellulose and hemicellulose polysaccharides, and aromatic moieties of lignin represent versatile raw materials for high value-added chemical synthesis.[43]

1.2 Levulinic acid production

As one of the BCBBs highlighted by Werpy and Petersen in 2004,[33] levulinic acid (LA) *(Figure 5)* is the platform chemical to produce a great number of bio-chemicals such as succinic acid, resins, polymers, pharmaceuticals, food flavoring agents, herbicides, plasticizers, solvents, and anti-freeze agents.[44]

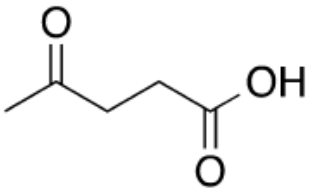

Figure 5: LA molecule.

LA (4-oxopentenoic acid; 5-ketovaleric acid) is a five carbon molecule with two different functional groups: a carboxylic unit and a ketone one. These two moieties endow the compound with interesting reactivity pathways.[45]

Both increasing number of scientific papers relating LA chemistry and the development of a wide range of products as its derivatives show the importance of LA in biorefinery concept.[46,47]

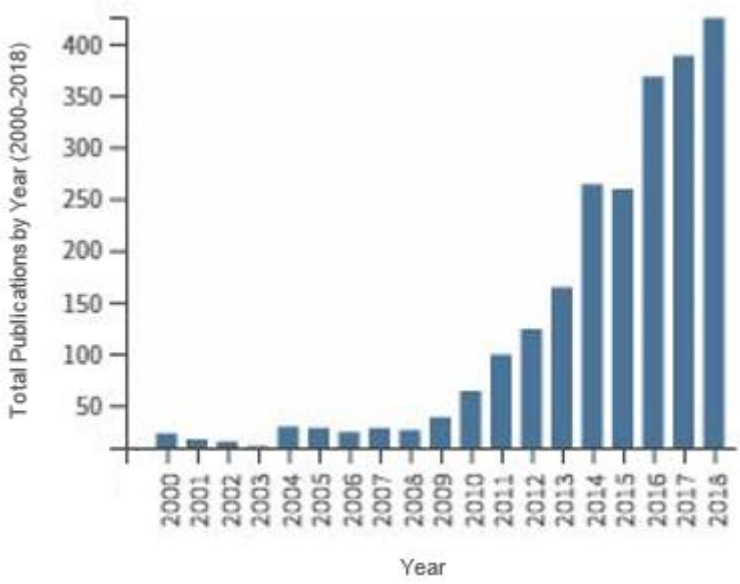

Figure 6: Number of publications on LA annually from January 2000 to December 2018.[46]

Global LA market demand was 2606 tons in 2013 and it is estimated to be 3820 tons by 2020. In 2013 the segmentation of LA market was estimated on the basis of its applications as follows: agriculture 42,8 %, pharmaceuticals 23.3 %, food additive 21 % and cosmetics 13 %.[48]

Some LA derivatives can be used for fuels and oxygenated oil additives. LA can undergo esterification with C1–C2 alcohols to form levulinate esters which can be applied in the flavouring and fragrances industries and as fuel additives.[49] In the presence of a bifunctional catalyst LA can be hydrogenated to produce methyl-tetrahydrofuran (MTHF), which can be employed as a gasoline blendstock.[50]

Furthermore, catalytic transformations of LA can lead to the production of strategic chemical commodities such as substituted pyrrolidones and lactones.[51] For instance, LA can undergo hydrogenation with molecular hydrogen or formic acid to produce γ-valerolactone (GVL),[50,52] which was proven to be a sustainable liquid transportation fuel suitable of replacing ethanol in gasoline–ethanol blends.[53] Continued hydrogenation of GVL produces valeric acid which in turn can be esterified with alcohols to produce a new class of cellulosic transportation fuels, known as ‘‘valeric biofuels’’.[54] *Bond et al.* developed an integrated catalytic process to convert GVL to liquid alkenes (ranging from C8 to C24) which could be blended with gasoline, diesel or jet fuels.[55]

Ketals of LA are studied as a source of new biobased monomers and polymers for applications as solvents, thermoplastics and polyurethanes.[56]

The conversion of LA into diphenolic levulinic acid (DPLA), a potential green replacement for bisphenol A in the production of polycarbonates, is widely investigated too.[57]

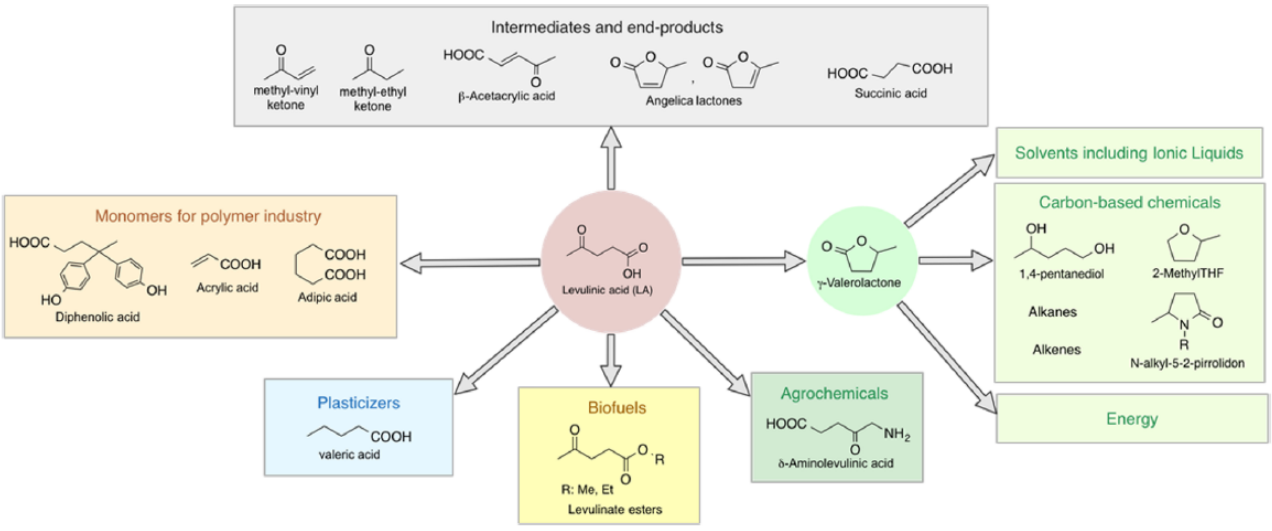

Figure 7: Chemicals derived from LA.[37]

1.2.1 Levulinic acid synthesis

LA can be synthetized in different processes, which include a five-step petrochemical route using maleic acid as key intermediate, a biocatalytic route from glucose, and the most important one: the acid catalyzed multistep conversion of polysaccharide content of biomass.[37]

Through biomass conversion, hemicellulose and cellulose can be hydrolyzed into their monomer units which constitute more active and accessible compounds for the obtainment of strategic chemical platform molecules.[58] Thus, considering the possible downstream chemical processing technologies of biomass upgrading, the conversion of sugars to value-added chemicals is fundamental.[59]

Hexoses, the six carboned sugars, are the most abundant monosaccharides existing in nature. Among them D-fructose and D-glucose represent indeed the most attractive chemical feedstocks and many research works have been devoted to their use as model substrates for catalytic transformations.[60]

Particularly, the acid catalyzed dehydration of C_6-monomers is a highly attractive processing reaction, because of the significant market potential of the resulting 5-hydroxymethilfurfural (5-HMF) as key intermediate for both the replacement of oil-derived chemicals and the development of novel products.[61]

It was found that both the dehydration rate of fructose and its yield and selectivity towards the synthesis of 5-HMF are higher, with respect to the use of other hexoses, under the same reaction conditions.[62]

Nonetheless, the use of the most abundantly available and cheaper glucose as chemical feedstock is one of the significant targets in the research field of biomass valorization.

Considering glucose as starting feedstock, the reaction for LA production proceeds through a complex mechanism, including isomerization of glucose to fructose followed by dehydration of the ketose monomer to 5-HMF and the subsequent rehydration of the furfural compound to form LA and an equivalent of formic acid.[63]

Overall, there are four parallel pathways in which glucose can react: reversion reactions leading to the formation of cellobiose and levoglucosan, degradation reactions, epimerization reaction to produce fructose and mannose, and dehydration to form 5-HMF. (*Figure 8*)[45]

Typical degradation products of catalytic sugar transformations are humins, namely highly polymerized carbonaceous species. These species can be both water soluble and water insoluble; water soluble ones polymerize with time to form water-insoluble compounds.[64]

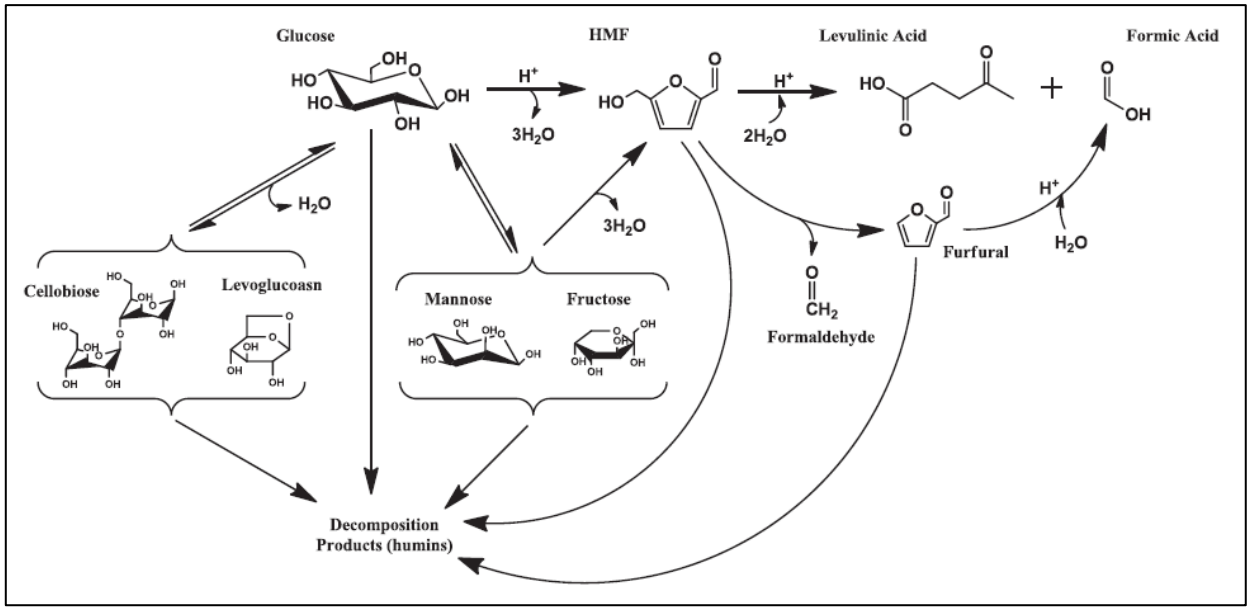

Figure 8: Reaction scheme of glucose hydrolysis.[45]

Glucose in an aqueous medium exhibits three conformers: a pyranose ring, a furanose ring, and an aldohexose open chair structure.

The higher reactivity of fructose, than glucose, renders the former a strategic target for the catalyzed isomerization of the latter.[65] Starting with glucose, the aldose (glucose)-to-ketose (fructose) isomerization step is necessary. The overall reaction network is complicated due to side reactions such as the epimerization of glucose to mannose, the retroaldolization of glucose to glycolaldehyde and erythrose, and the fructose conversion to glyceraldehyde and dihydroxyacetone.[16] (*Figure 9*)

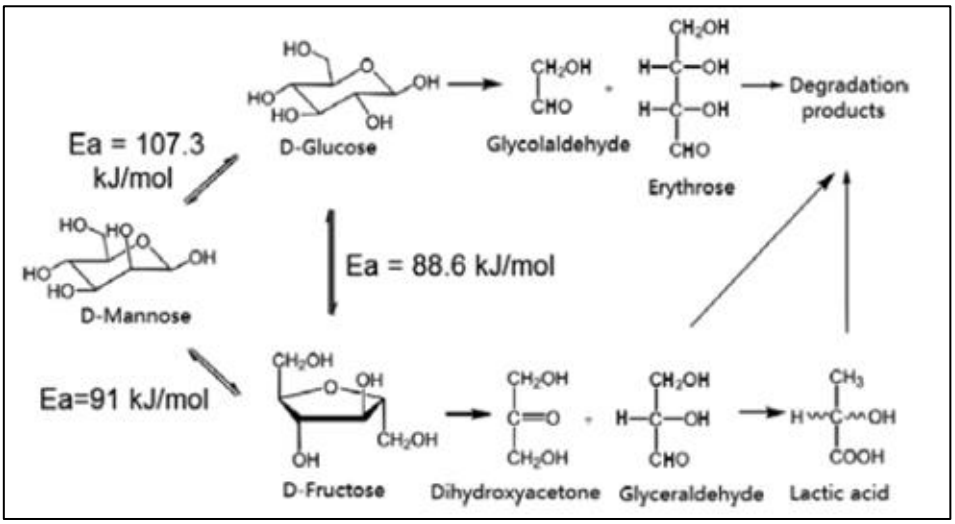

Figure 9: Glucose isomerization reaction network.[16]

Kinetic studies regarding glucose isomerization reveal that, as the energy barrier from glucose to fructose is 17% lower than that to mannose, fructose is the major isomeric product under appropriate kinetic control.[66]

The isomerization of glucose to fructose can occur in acidic conditions and it has been reported that the reaction is favored by the presence of Lewis acid sites.

Inorganic Brønsted bases can also catalyze the glucose isomerization reaction, albeit with low yields, because of the reduced stability of monosaccharides in the presence of basic catalysts.[67] Isomerization reactions can be catalyzed in the presence of immobilized enzymes as well. The reaction catalyzed by xylose isomerase is the largest biocatalytic process utilized on an industrial scale and it is employed to produce high-fructose corn syrups (HFCS), which represent a cheap source of fructose. The equilibrium-based, maximum thermodynamic yields of fructose is 57.4 % at 100 °C.[68]

After the isomerization reaction, the subsequent step is the transformation to 5-HMF which is an important precursor for the synthesis of a variety of commodity chemicals and fuels.[69] 5-HMF production by multistep dehydration of fructose is catalyzed by both Lewis and Brønsted acid sites. Before the 1980's the 5-HMF synthesis was almost exclusively focused on the homogeneous acid-catalyzed transformation of C6-sugars in water as a commonly and frequently employed solvent for carbohydrate chemistry. Nonetheless, in the last decades, different catalytic systems, both homogeneous and heterogeneous types, and alternative solvents such as ionic liquids, common organic solvents and various combinations of them, have been widely studied.[70]

As already mentioned, 5-HMF is a strategic intermediate for the synthesis of various value-added chemical compounds. For instance, it can undergo hydrogenation to 2,5-

dimethylfuran or etherification to 5-ethoxymethylfurfural, as promising liquid fuels, or it can be oxidized to 2,5-furandicarboxylic acid (FDCA) which can replace oil-derived terephthalic acid. Undoubtedly, another important strategic compound produced through 5-HMF intermediate, is levulinic acid (LA).[71,72]

Nowadays, the synthesis of 5-HMF is preferably performed in organic solvent and other reaction media.[70] Instead, water was found to be the best solvent for LA synthesis.[37] Therefore, as 5-HMF is an intermediate in the reaction sequence, the overall yields of LA are lower than those regarding 5-HMF production. Moreover, the chemistry process of LA production is operated at higher acid concentration, leading a higher formation of humins.[73] Furthermore, while 5-HMF is produced from fructose on both Lewis and Brønsted acid sites, LA from the furfural intermediate is produced exclusively on Brønsted sites.[45]

Focusing on molecular mapping of conversion of 5-HMF to LA, recently it has been found that the most favorable reaction route is that reported in *Figure 10*.[74]

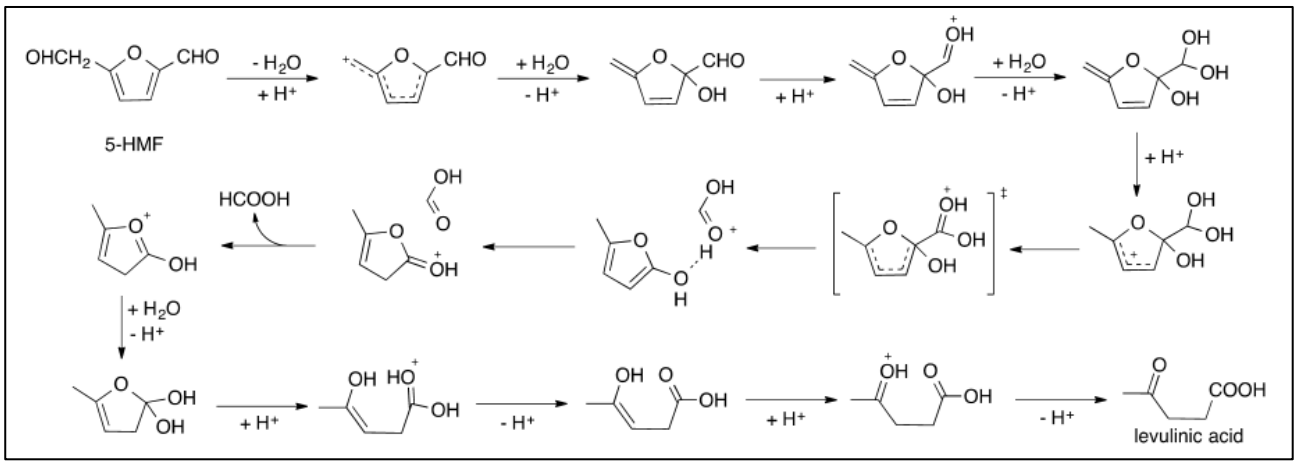

Figure 10: Reaction route of 5-HMF conversion to LA.[74]

1.2.2 Catalysts for levulinic acid production

As previously seen, the formation of LA from glucose conversion involves a series of complex reactions which require different types of chemical active functionalities. Nevertheless, the most important process by which LA can be obtained consists of an acid catalyzed one-pot and multistep approach.[37]

Chemocatalytic conversion can be classified into homogeneous and heterogeneous reactions.

Industrially, the obtainment of LA from sugary feedstocks is achieved using homogeneous catalysts, specifically strong mineral acids.

Homogeneous Brønsted acid catalysts such as H_2SO_4, HCl, HNO_3 and $HClO_4$ are widely employed both in raw biomass hydrolysis reactions and in carbohydrates conversion processes, because of favourable yields with reasonable costs.[75]

The production of LA from cellulosic feedstocks including wood waste and agricultural residues, employing sulfuric acid as a catalyst, was developed in the 1980's by Biofine Renewables and commercialized in the 1990's.[76] The homogeneous catalytic process has been applied in the first biorefinery in Caserta, Italy, and it is known as the "Biorefine process".[77] It involves a continuous process constituted by two reactors in order to minimize side product formation.[76] Through this process, LA is produced with yields between 60 and 70 % of the theoretical yield based on the hexose content of the cellulosic material.[59]

Nonetheless, despite their cheap nature and their catalytic efficiency, the use of mineral acids entails various hurdles, including reactor corrosion, difficulty to separate the products, waste generation and energy-intensive processes to recycle the catalysts; indeed, their practical applications raise serious environmental concerns.[78]

Therefore, the development of heterogeneous catalysts for biomass valorization processes has attracted great interest.[79] The numerous advantages related with the use of solid catalysts include the catalysts recyclability and the easy separation from the reaction mixture, thus avoiding neutralization and extraction steps, and reducing the waste formation. Indeed, tailored solid catalyst features may improve the yield and the selectivity toward the desired product.[80]

Therefore, heterogeneous catalysts appear as a promising sustainable alterative to currently employed homogeneous catalysts and in this regard various systems have been explored.

Metal oxide from Group IV and V have attracted extensive interest in the development of solid catalysts for aqueous-phase transformation of sugars due to unsaturated coordination of metal species as water-tolerant Lewis acid sites.[81] Exposed oxygen-deficient cations of metal oxides act as Lewis acid centers, while hydroxyl groups are responsible for the Brønsted acid sites.[82] Nonetheless, the study of metal oxides as catalysts has been limited almost to the production of 5-HMF and the production of this platform chemical from glucose over aqueous medium was often less than 15% yield by bare metal oxides including γ-Al_2O_3, SiO_2/Al_2O_3, TiO_2, ZrO_2, ZrO_2/TiO_2, so that the acidity of these solid catalysts is not enough to drive the reaction toward the desired product.[83]

Indeed, the most explored heterogeneous catalysts for LA production from glucose are ion-exchange resins and zeolites. However, both systems own downsides.

Ion-exchange resins are insoluble polymeric materials that are capable of exchanging certain ions inside their structure with others in the reaction mixture. Sulfonated ion-exchange resins are employed as Brønsted acid catalysts, and they are typically co-polymers of styrene and divinylbenzene tailored with acid active sites (i.e., -SO_3H groups). Amberlyst, Nafion and Dowex have been widely applied for sugar conversion reactions.[84, 85] Nevertheless, the ion exchange resins usually suffer from poor thermal stability (~150°C) and difficulty in removing the adsorbed substrate, which limited the reuse of the catalyst in multiple cycles.[86,87]

Zeolites as catalysts for lignocellulosic-derived-sugar containing feed streams valorization has been widely explored, too.[88,89] The coordinatively unsaturated cations in zeolites act as Lewis acids, while highly polarized hydroxyl groups behave as Brønsted acids.[90] Impregnating appropriate amount of $FeCl_3$ on HY zeolite (Fe/HY zeolite) has demonstrated both an increased number of total acid sites and an enlargement of the pore size to produce larger amount of LA in aqueous medium than the parent HY zeolite (LA yield 62%).[91] However, the small and narrow pore dimension of zeolites, limits the reactivity to external surface of the catalysts, thus hampering catalytic efficiency due to limited access and diffusion limitation to the active sites.[92] Indeed, pore obstruction is another limit for these materials due to their small pore dimensions.[93] All these aspects make zeolites suitable acid catalysts for sugar conversion but hinder their use if actual raw biomass is employed as feedstock.[94] Indeed, mass transfer limitation between bulky biomass substrates and zeolites prevents their upscale utilization.[95]

In order to address the above-mentioned issues, Ordered Mesoporous Silica materials (OMS) may stand for environmentally benign and economically feasible catalytic frameworks for LA production.

1.3 Ordered Mesoporous Silica catalysts

“Liquid crystal templating” (LCT) is a method used to synthesized ordered mesoporous materials, whose strategic properties as catalysts are industrially exploited.[96,97] This technique was independently used in 1990 by researchers in Japan,[98] but became notorious just a couple of years later, when scientists at Mobil Corporation discovered a family of silicate and aluminosilicate mesoporous ordered materials prepared via LCT method.[99] These materials started to be produced at Mobil Corporation Laboratories with the name M41S. The synthesis of this family of mesoporous materials is based on the combination of

two major topics, sol-gel technique and surfactant (templating) science. Template agents are amphiphilic molecules, which under proper conditions, can form self-assembled surfactant molecular arrays, which can organize in ordered mesophases. Combination of metallic precursors and structure-directing agent can give rise to mesoporous materials denoted by uniform pore sizes in the range 2-10 nm or higher. (*Figure 11*)[100]

Therefore, LCT method consists in a highly versatile synthetic approach.

Common features of Ordered Mesoporous Silica are: high specific surface areas which allow to have high concentration of active sites upon the material surface, ordered porous structures with amorphous silica walls , and larger pore dimensions compared to zeolitic materials and MOFs, which facilitate reactant and product diffusion. Furthermore, due to superficial silanol groups, OMS bears a low intrinsic Lewis acidity.

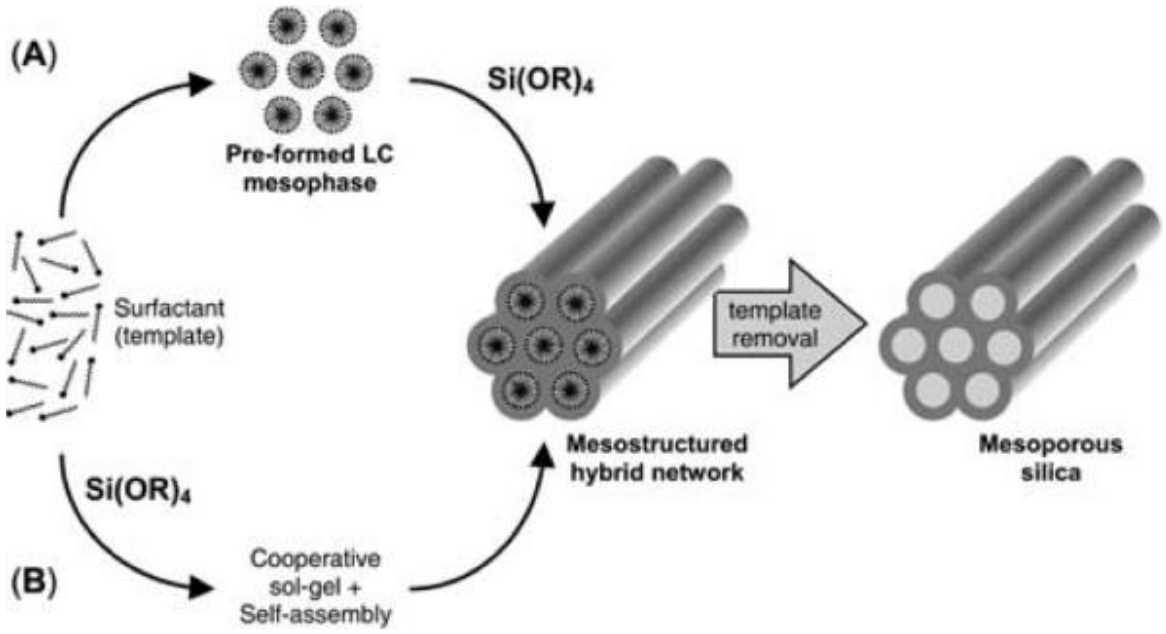

Figure 11: Schematic pathway for preparing surfactant-templated mesoporous silicas.[100]

In addition to M41S', among which MCM-41 is the most known, other OMS have been developed such as the SBA-types. These supports are particularly interesting because both their high specific surface areas and ordered pore structures are comparable to the ones of M41S'. However, some of their properties may result more attractive for their possible application in this work. Particularly, the attention will be focus over the SBA-15 as a pliable substrate in order to develop new active heterogeneous catalysts for LA production.

1.3.1 SBA-15 and its possible modifications

Figure 12: SBA-15.

In 1998 researchers at the University of California, Santa Barbara, developed a novel type of mesoporous material which named Santa Barbara Amorphous No. 15 (SBA-15).[101] The structure of SBA-15 is characterized by a bidimensional hexagonal array of pores exhibiting a *p6mm* symmetry, like the one of MCM-41, and a large specific surface area (≥700 $m^2 \cdot g^{-1}$). SBA-15 synthesis was developed by Zhao[102] and it requires a strongly acidic media (pH ≤ 2) as reaction environment and the use of a polymeric neutral surfactant as structural directing agent.[103] Indeed, the template used is a linear triblock copolymer of poly(ethylene oxide)$_n$-poly(propylene oxide)$_x$-poly(ethylene oxide)$_y$, (PEO)$_n$-(PPO)$_x$-(PEO)$_y$, commercially known as Pluronic P_{123}. The use of non-ionic templates involves advantages from both an environmental and economic point of view.[104] Water solubilization of this polymer is due to the formation of hydrogen bonds between water molecules and alkyl oxide polymer units. In an acidic environment, P_{123} solubility is also enhanced by H_3O^+ ions, which favor inorganic precursor-templating agent interactions. Working within a pH lower than the silica isoelectric point (pH~2) leads silica to be positively charged and causes the formation of a composite inorganic-polymeric mesophase which involves electrostatic interactions.[105]

Both MCM-41 and SBA-15 are characterized by a highly regular array of uniform-sized channels deriving from an hexagonal type mesophase, but MCM-41 owns smaller average pore diameters (2.5-3nm), compared to that of SBA-15 (5-10nm).[106,107] Relatively large pore sizes compered to MCM-41 provide SBA-15 with high potential to better interact with bulky reactants as those coming from cellulosic feed-streams. Therefore, larger pores dimensions of SBA-15 represent a good way to overcome mass transfer limitations, allowing the upscale employment of this catalyst for biomass valorization.

Despite favorable characteristics of SBA-15, this support itself owns two major drawbacks concerning the stability characteristics and the acidic properties, respectively.

Concerning the first aspect, the catalyst robustness is too low under the required hydrothermal conditions (180-200 °C), with the result that no catalyst can be recovered at the end of the reaction. As regards the acidity concept, instead, the material intrinsic acidity is not enough to provide activity toward the obtainment of LA, so that the lack of Brønsted acidity strongly affects the catalytic performance.

Therefore, in order to achieve the desired catalytic properties, the SBA-15 system has to be properly tailored operating toward both these two aspects.

Various approaches can be resorted on to modify the morphological and chemical-physical SBA-15 features.

Many works have been reported in literature regarding the synthesis of various silica-metal SBA15-type composites.[108] In that way, the approaches can be of direct synthesis, mainly consisting of co-condensations methods, or of post-synthesis type, as the grafting technique or incipient wetness impregnations.[109,110] With the aim of providing robustness to the silica support, one of the most investigated oxide promoter for SBA-15 is the Niobium oxide, which can furthermore enhance the acidic property.[111] However, one of the major drawback of this promoter is its high cost. In order to overcome both the acid and stability lack, Al has been also widely investigated as SBA-15 co-support.[112,113] Due to the overabundance of literature regarding the Al use for silica support modifications, the attention of this work has been devoted to another Lewis acid metal, which may well interact with the silica matrix.

Therefore, considering the stability aspect, in order to overcome the SBA-15 lack of both hydrothermal and mechanical stability, the silica support has been modified by the introduction of titanium dioxide as structural promoter. TiO_2 was chosen due to its cheap nature and stronger mechanical stability with respect to the silica material. So far, silica-titania composites have been studied especially as photocatalysts,[114] but also for other applications such as catalytic oxidations[115] as well as for biomedical purposes.[116]

In order to provide strong acid active functionalities to the support, the most common technique is to add sulfonic group via direct sulfonation method.[117] Sulfonic acid loadings over silica-based heterogeneous catalysts have been achieved with one-pot co-condensation approaches.[118] However, the direct synthesis method in many cases leads to loss of mesoscopic order of the pore architecture. Indeed, it is usually carried out in a concentrated sulfonic acid with heating.[119]

An effective alternative to the direct sulfonation method is the grafting technique. It consists of a post synthesis strategy, by which the active functionalities are anchored on the support surface via covalent bonds. (*Figure 13*) Particularly, the hydrothermal saline promoted

grafting approach represent a more sustainable way in order to provide the catalyst with the needed moieties.[120]

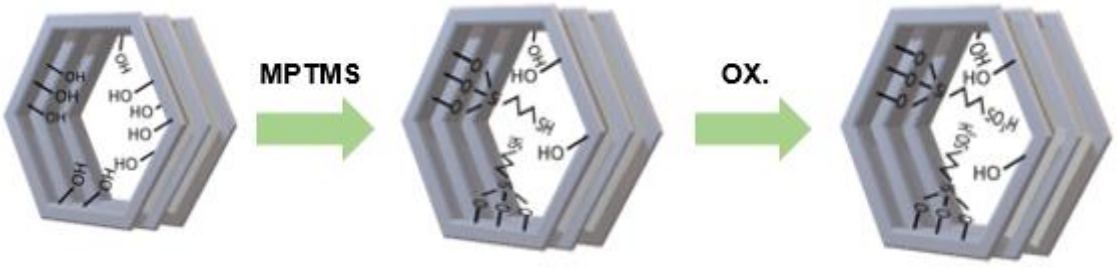

Figure 13: Acid functionalities grafting technique representation.

2. AIM OF THE WORK

This work focuses on the development of a stable, robust and active heterogeneous catalyst for the glucose hydrolysis in order to obtain LA, an important biobased building block.

Due to its morphological and structural properties, SBA-15 has been chosen as catalytic substrate. Nevertheless, the major drawbacks of this Ordered Mesoporous Silica for these kinds of applications are its lack of both the stability and the acidity characteristics. Therefore, focusing on these two different issues, deep modifications of the silica pristine material have been performed: on the one hand in order to develop a robust catalytic system and on the other with the purpose of providing the support with the needed active functionality.

Considering the stability aspect, SBA-15 has been tailored by the introduction of titanium dioxide as co-support. Particularly, two different synthesis procedures and various Ti amounts have been taken into account.

In order to improve the acidity of the catalyst, the best synthetized support has been functionalized by an innovative post-grafting method, which includes the use of MPTMS as grafting agent and the economic and sustainable NaCl aqueous medium as reaction solvent.

In order to evaluate the physical and chemical properties of the synthesized materials, an in depth characterization has been carried out by using different and complementary techniques.

With the aim of investigating the activity of the grafted catalyst, it has been tested under batch conditions for the hydrolysis of glucose and fructose in an aqueous medium. Reactivity parameters, such as product yields, selectivity and carbon balance, have been evaluated and compared to that of another acid heterogeneous catalytic system.

3. MATERIALS AND METHODS

3.1 Synthesis

3.1.1 Synthesis of SBA-15

Reagents:

- *Tetraethyl orthosilicate ($SiOC_2H_5)_4$, assay: 98%, Sigma-Aldrich*
- Poly(ethylene glycol)-block-poly(propylene glycol)-block-poly(ethylene glycol), (Pluronic, P_{123}), average M_n ~5,800, Sigma-Aldrich
- *Hydrochloric acid (HCl), assay: ≥37%, Sigma-Aldrich*
- *Deionized water*

SBA-15 synthesis was performed following Zhao's protocol[102] with some modifications.
The molar composition of initial gel was 0,0175 P_{123}: 1 TEOS : 6 HCl : 42,5 H_2O.
Pluronic P_{123} triblock copolymer was added in 300 mL of 2 M HCl solution. In order to hasten the polymer dissolution, first the system was sonicated for 90 minutes at 45 °C. Secondly, the solution was cooled at room temperature and stirred until the template was completely dissolved. The tetraethyl orthosilicate (TEOS) was subsequently added dropwise into the stirred solution with a rate of 0,3 mL/min by means of a peristaltic pump. The solution was maintained at room temperature for 20 hours under stirring. Then, it was transferred in a Teflon bottle to perform a hydrothermal treatment at 90 °C for 42 hours, under autogenous pressure and a static condition. The solid precipitates were collected by filtration, washed several times with deionized water and dried at 80 °C overnight.
Finally, the solid product was grinded, and the resulting powder was calcined in air (50 mL/min) at 550 °C for 6 hours, with heating rate of 1 °C/min, to remove organic template. The thus prepared pristine silica support was simply named SBA-15.

3.1.2 Synthesis using the Ti salt

Reagents:

- *Tetraethyl orthosilicate ($SiOC_2H_5)_4$, assay: 98%, Sigma-Aldrich*
- Poly(ethylene glycol)-block-poly(propylene glycol)-block-poly(ethylene glycol), (Pluronic, P_{123}), average M_n ~5,800, Sigma-Aldrich
- *NaCl, assay: 99,8%, BAKER ANAYZED®*
- *Titanium(IV) isopropoxide ($Ti[OCH(CH_3)_2]_4$, assay: 97%, Sigma-Aldrich*
- *Hydrochloric acid (HCl), assay: ≥37%, Sigma-Aldrich*
- *Deionized water*

The silica-titania composites were prepared by a co-condensation method based on the gel composition of 0,013 P_{123}: 1 TEOS : 1 NaCl : 0,05-0,15 $TiOCl_2$: 0,025-0,5 HCl : 220 H_2O.
The synthesis was performed using a method reported earlier,[116,121] with some modifications. TEOS and titanium oxychloride ($TiOCl_2$) were used as silica and titania precursors, respectively, in the presence of triblock copolymer P_{123}, as a structure-directing agent.
Pluronic P_{123} was added in 238 mL of water in which NaCl was previously dissolved. Ultrasounds were applied for 90 minutes at 45 °C to favour the polymer dissolution. After this step, the solution was cooled at room temperature and stirred until the template was completely dissolved. Then, TEOS was poured into the polymer solution dropwise under magnetic stirring. TEOS was pre-hydrolyzed in this solution for 210 minutes before addition of titania precursor, which was meanwhile prepared in situ. Titanium oxydichloride was synthetized by carefully adding titanium(IV) isopropoxide to concentrated hydrochloric acid at 0 °C in a 2-necked round bottom flask (250 mL) connected with a cooling condenser. The solution was kept under vigorously stirring for 1 hour in an ice-bath (*Figure 14*). Afterwards it was filtered, thereby obtaining a transparent yellowish solution. The Ti salt acid solution was added dropwise to the TEOS synthesis solution and the reaction mixture was aged at room temperature for 20 hours. Then, it was transferred in a Teflon bottle to perform a hydrothermal treatment at 90 °C for 42 hours, under autogenous pressure and a static condition. After that, the solid precipitate was filtered off, intensively washed with deionized water and kept drying at room temperature.
Finally, the solid product was grinded, and the resulting powder was calcined in air (50 mL/min) at 550 °C for 6 hours.

The resultant materials were designated as %Ti-SBA15, where % = 5, 10 or 15 is the Ti molar amount in the gels.

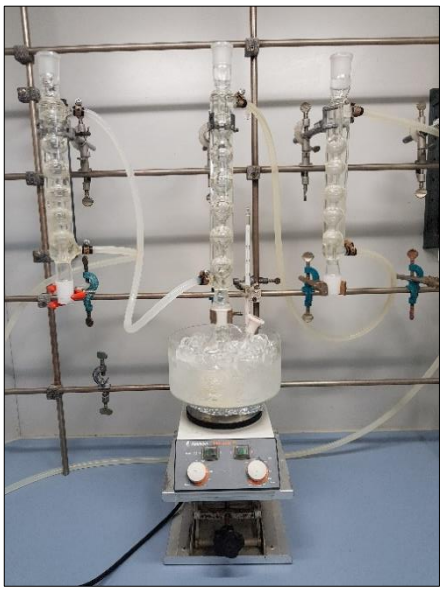

Figure 14: In situ preparation of the Ti-salt.

3.1.3 Synthesis using Acetylacetone as chelating agent

Reagents:

- *Tetraethyl orthosilicate ($SiOC_2H_5)_4$, assay: 98%, Sigma-Aldrich*
- Poly(ethylene glycol)-block-poly(propylene glycol)-block-poly(ethylene glycol), (Pluronic, P_{123}), average M_n ~5,800, Sigma-Aldrich
- *Titanium(IV) butoxide (Ti ($OCH_2CH_2CH_2CH_3)_4$), ($Ti(Bu)_4$), assay: 97%, Sigma-Aldrich*
- *1-Butanol ($CH_3(CH_2)_3OH$), assay: ≥99,5%, Sigma-Aldrich*
- *Acetylacetone ($CH_3COCH_2COCH_3$), assay: ≥99%, Sigma-Aldrich*
- *Hydrochloric acid (HCl), assay: ≥37%, Sigma-Aldrich*
- *Deionized water*

The titania-loaded SBA-15 composites were prepared by a co-condensation method based on the gel composition of 0,0175 P_{123}: 1 TEOS : 0,05-0,15 $Ti(OBu)_4$: 6 HCl : 42,5 H_2O.

Titanium(IV) butoxide was used as titanium precursor. It was added to the silica synthesis solution after reaction with acetylacetone (AcAc) as chelating agent, in order to slow down its hydrolysis rate. Triblock copolymer P_{123} was used as templating agent.
The procedure for the preparation of the silica aqueous solution was similar to the SBA-15 method. Titanium(IV) butoxide was added to a solution containing the chelating agent and 1-Butanol solvent. The molar ratio of $Ti(OBu)_4$/AcAc/BuOH was 1 : 0,49 : 4,20; the titanium solution was maintained under stirring for 1 hour. The thus prepared titanium solution was added dropwise to the sol made of TEOS and P_{123}. The reaction mixture was kept at room temperature for 20 hours. Then, it was sealed in a Teflon bottle and hydrothermally treated at 90 °C for 42 hours, under autogenerated pressure and a static condition. After this step, the solid product was filtered with a Gooch funnel, abundantly washed with deionized water and dried at room temperature.
The as-made samples were named %TiAcAc, where % = 5, 10 or 15 corresponds to the Ti molar amount in the gels.

3.1.4 MPTMS grafting and oxidation

Reagents:

- *(3-Mercaptopropyl)trimethoxysilane ($HS(CH_2)_3Si(OCH_3)_3$), assay: 95%, Sigma-Aldrich*
- *NaCl, assay: 99,8%, BAKER ANAYZED®*
- *Hydrogen Peroxide Solution (H_2O_2), 30 wt. % in H_2O Sigma-Aldrich*
- *Deionized water*

The best silica-titania support was functionalized with propylsulfonic acid by post-grafting method.[120] The approach includes a mild hydrothermal treatment in an aqueous solution of NaCl, which furthermore represents an economic and environmentally friendly solvent with respect to common grafting solvents such as chloroform, toluene and hexane.[122,123] The possible role of H_2O/NaCl in activating siloxane bridges for grafting is reported in *Figure 15*.

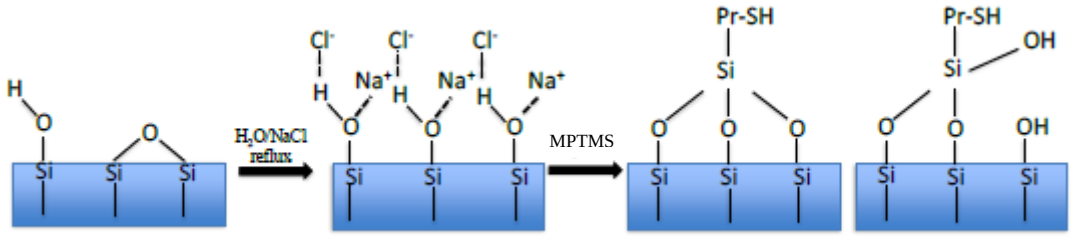

Figure 15: Possible role of H_2O/NaCl in activating siloxane bridges for grafting.[120]

The molar ratio employed for the grafting reagents was: 1 SiO_2 : 5 NaCl : 2 MPTMS : 0,02 H_2O.

The support was mixed for 15 minutes in a pre-synthetized saline aqueous solution of NaCl. Then, the organosilane grafting agent (MPTMS) was added. The suspension was refluxed at 90 °C under stirring for 24 hours. After filtration of the resulting thiol-functionalized solid, it was washed three times with deionized water and dried overnight at 70 °C. The grafted catalyst was labeled %SB-SH.

After this step, thiol groups were converted into the -SO_3H moieties by mild oxidation with 30% hydrogen peroxide by continuous stirring at 30 °C for 24 hours. The molar ratio used for the oxidation was SiO_2/H_2O_2 1 : 0,11. The sulfonated solid product was subsequently filtered, washed with methanol using a centrifuge and dried at RT.

The resulting acid catalyst was called SB-SO_3H.

3.2 Characterizations

The following characterization techniques were used to investigate physicochemical properties of the synthesized samples.

3.2.1 Nitrogen Physisorption

Nitrogen physisorption gives information concerning surface area, pore volume, pore size distribution and pore shape. This technique relies on non-selective absorption of gas molecule (adsorbate) on a solid surface (adsorbent) through weak interactions.[124] Depending on the predominant pore sizes, the porous solid materials are classified by International Union of Pure and Applied Chemistry (IUPAC) as:[125]

- Microporous, with pore diameter smaller than 2 nm
- Mesoporous, with pore diameter between 2 and 50 nm
- Macroporous, with pore diameter larger than 50 nm

Since heterogeneous catalysis is a surface phenomenon, the knowledge of catalysts' morphological properties such as surface area and pore size, is essential to understand the correlation between the catalytic performance and the physicochemical aspects.
The most used technique is nitrogen physisorption, relying on absorption and desorption of nitrogen at -196 °C.[126] Plotting the total amount of adsorbed (or desorbed) gas at a given value of relative pressure (p/p_0), yields a response called adsorption isotherm.
IUPAC classifies six types of isotherms, according to different materials. (*Figure 16*)

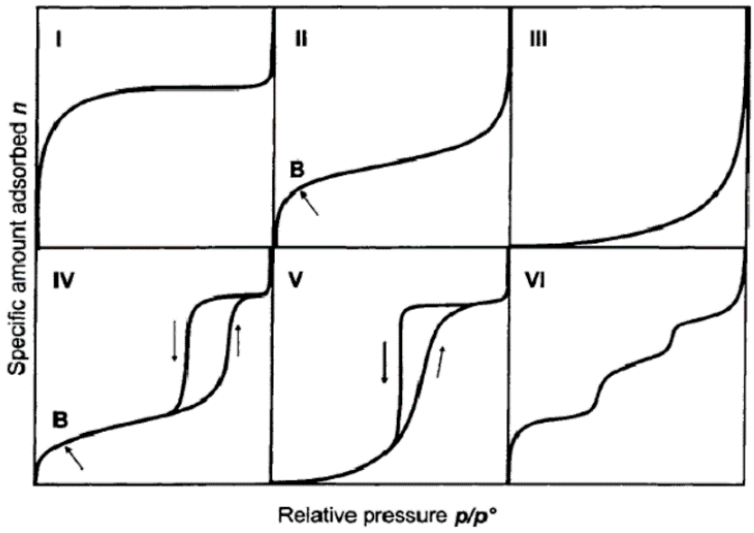

Figure 16: IUPAC classification of adsorption isotherms.[127]

Type I isotherm is typical for microporous materials. Type II regards non-porous or macroporous systems. Type IV is the most common and related to mesoporous material, displaying the typical hysteresis reported in *Figure 16*. Type III and V are usually uncommon and indicate weak adsorbate-adsorbent interaction on macroporous or mesoporous materials, respectively. Type VI is related to flat surface with no porosity, showing a layer-by-layer adsorption.
Physisorption values were recorded using a Tristar II Plus Micromeritics. Before starting the analysis, the sample (100 mg) was thermally treated in vacuum at 200 °C for 2 hours in order to remove all adsorbed species. Surface area information was taken in 0,05-0,35 p/p_0

range, where no capillary condensation occurs. Surface area is calculated knowing the adsorbed nitrogen monolayer volume (*Vm*), through *Equation 1*. *NA* is the Avogadro number ($6{,}023 \cdot 10^{23}$), *22414* represent the volume (cm^3) of one mole of ideal gas in standard conditions, while σ represent the occupied surface area by one molecule of N_2, generally accepted to be 0,162 nm^2.[126]

$$A_s = \frac{V_m}{22414} N_A \sigma$$

Equation 1: Surface area equation.[126]

The monolayer adsorbed volume is calculated through the Brunauer, Emmet, Teller (BET) theory (*Equation 2*), whose fits experimental data only for P/P_0 lower than 0.35, where only physisorption occurs. V_{ads} is the adsorbed volume while *c* is the BET constant (related to adsorbate-adsorbent interaction).

$$\frac{p}{V_{ads}(p_0 - p)} = \frac{1}{V_m c} + \frac{c-1}{V_m c} \cdot \frac{p}{p_0}$$

Equation 2: BET equation.[128]

3.2.2 X-Ray Diffraction (XRD)

X-ray diffraction is widely employed in solid-state material characterization. This technique enables to get information concerning crystal phases and their relative abundance, crystallite sizes and distortion of the crystal lattice.

In this work XRD analyses were performed to determine the samples structure after calcination.

X-rays, due to their highly energy, are able to penetrate solid matter, since their wavelength is similar to atomic dimensions (10^{-3}-10 nm).[129] In any X-ray irradiated material, oscillation of electron inside the crystal occurs and part of the incident radiation is emitted. Due to ordered structure of scattering atoms (periodic lattice), constructive and destructive interference arises, depending on the diffraction angle (θ): this is the diffraction phenomena. Each crystal phase is identified by a peculiar X-ray diffractogram, a pattern in which intensity of scattered rays is plotted against 2θ.

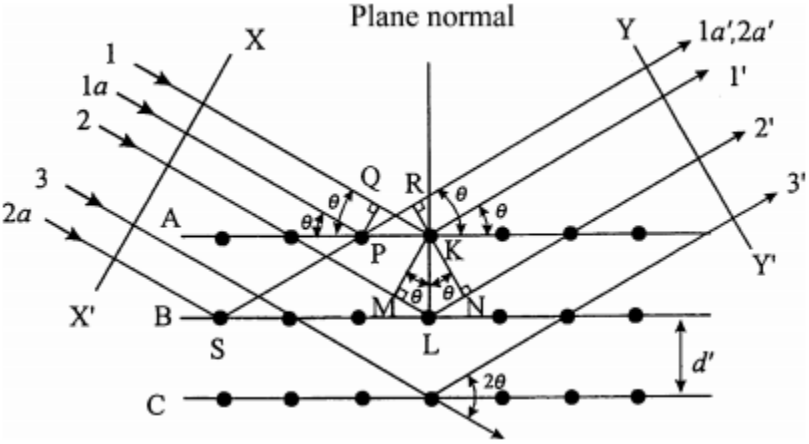

Figure 17: Representation of X-ray scattering by a crystal.[129]

A correlation between diffraction angle (θ) and atom spacing (d_{hkl}) between two crystallographic planes with the same Miller indexes (*h*,*k*,*l*) (*Figure 17*) is given by the Bragg's law (*Equation 2*). *λ* is the wavelength of incident radiation and *n* is the order of diffraction.

$$n\lambda = 2d_{hkl}\sin\theta$$

Equation 3: Bragg's law.[130]

From plane spacing (d_{hkl}) it is possible to calculate the lattice constants (*a*, *b*, *c*) and the volume, whose knowledge is useful to understand possible lattice distortion.
Crystallite sizes (*t*) can be determined through the Scherrer formula (*Equation 4*). *K* is a constant that depends on the peak's shape, *λ* is the wavelength of incident radiation, *θ* is the diffraction angle and *β* is the full width at half maximum intensity.

$$t = \frac{K \cdot \lambda}{\beta \cdot cos\,\theta}$$

Equation 4: Scherrer equation.[130]

Wide angle x-ray scattering (WAXS) was used to obtain this information.

The powder XRD measurements were performed in the Department of Earth Science at the University of Ferrara thanks to Professor Giuseppe Cruciani collaboration. The analyses were carried out using a Bruker D8 Advance powder diffractometer with $CuK\alpha_{1,2}$ radiation at an accelerating voltage of 40 kV and an applied current of 30 mA.

Instrumental parameters are reported below:

- Stepsize: 0,02 °
- Antiscatter: 1/2 °, 0,1 mm, 1/2 °
- 2θ range: 5-80 °
- Time/step: 3 s

3.2.3 Temperature Programmed Oxidation (TPO)

Temperature programmed oxidation is a technique that consists in monitoring oxidation reactions, while temperature increases linearly with time.[131] In this way the presence of oxidable species is detected. TPO is a common analysis among catalysts characterizations since it can give information about organic oxidizable residues on a solid material. These species may be wanted (e.g. C-doping), or undesirable (e.g. carbon coke deposits over used catalysts).

Operatively, 50 mg of the sample were placed in a U shaped quartz reactor and heated in a 5 % O_2/He gas mixture, 40 mL/min with a heating rate of 10 °C/min from 25 °C up to 800 °C. A trap was equipped with magnesium perchlorate and soda-lime to remove from the gas flow water and CO_2, respectively. Oxygen consumption, that is related to oxidation reactions, was monitored *via* a Gow-Mac thermal conductivity detector (TCD): when gas composition changed, i.e. oxygen was consumed, a signal variation took place. The instrumental output consists in a plot of temperature versus oxygen consumption.

The TPO technical apparatus is shown in *Figure 18*.

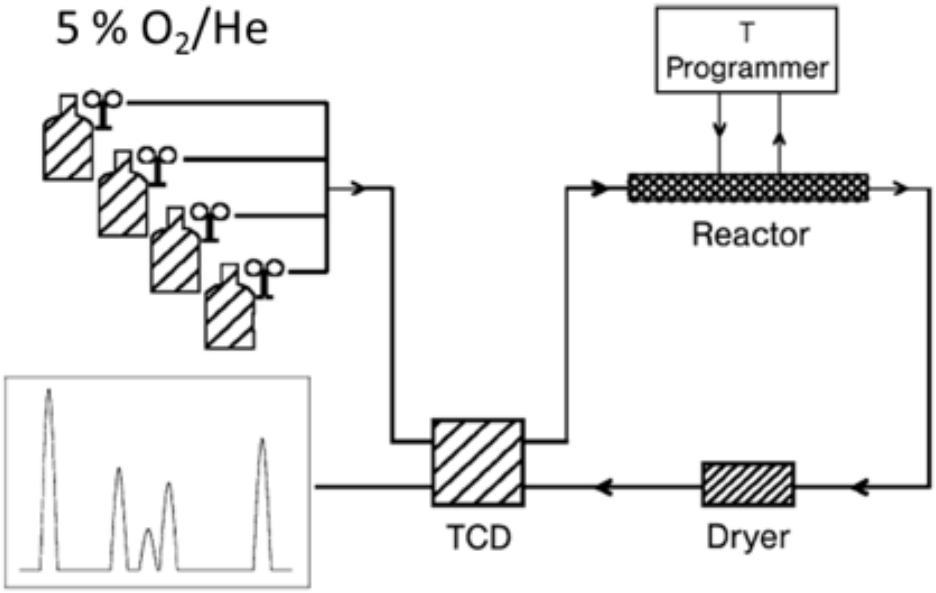

Figure 18: TPO analysis rig.

3.2.4 Titration method

The total Brønsted-acid sites of the grafted catalyst and that of the SBA-15 pristine material were determined by a titration method previously reported in literature.[132] A sodium hydroxide aqueous solution (0.002 M, 20 mL) was added to a catalyst (50 mg), and the mixture was stirred for 1 hour at room temperature. After filtration of the solid, the solution was titrated with a hydrochloric acid aqueous solution (0.002 M) to determinate the total acid density. The number of Brønsted-acid sites was estimated from the difference between the total amount of base and acid used during the titration, respectively. (*Equation 5*)

$$mol_x = mol_{base} - mol_{acid}$$

Equation 5: Titration formula used to calculate the total Brønsted-acid amount of the catalysts.[132]

3.3 Tests

In order to determine both the mechanical and the hydrothermal stability of the samples, as well as their catalytic activity for the glucose hydrolysis, various tests were carried out.

3.3.1 Mechanical stability tests

With the aim of investigating the mechanical stability of the catalysts, the supports' powders were pressed (5 metric ton·m^{-2}) for 5 minutes; the resulting tablets were subsequently crushed and sieved to mash size of 14-18 (1-1.4 mm).
The pressed samples were analyzed by physisorption and the results were compared with that of the pristine sample.

3.3.2 Hydrothermal stability tests

In order to evaluate the hydrothermal stability of the synthesized materials, the samples were examined under batch condition in an autoclave stainless still reactor. 100 mg of the samples in the mash size 14-18, were suspended in an aqueous medium at 200 °C for two hours, under autogenous pression in a N_2 inert atmosphere.
The solids were recovered by filtration and dried at 80 °C overnight.
The weight percentages of the recovered catalysts were taken into account in order to evaluate the stability of the systems under hydrothermal conditions.

3.3.3 Reactivity tests

The catalysts were tested in the glucose and fructose hydrolysis; batch tests were carried out in an autoclave stainless still reactor.
500 mg of substrate (*sub*) were analyzed with 200 mg of the catalysts (mash size of 14-18) in an aqueous medium at 180 °C for 5 hours, under 10 bar of N_2 inert atmosphere. Time of reaction started to be calculated when the autoclave temperature reached 180 °C.
The reaction solutions were analyzed via High-Performance Liquid Chromatography (HPLC) analysis. The chromatograph used was a Agilent Technologies 1260 Infinity II, equipped with a Aminex HPX-87H column, which was kept at a temperature of 50 °C during the

analyses. The mobile phase was 5 mM H_2SO_4 (rate flow 0,6 mL/min) and the analytes' signals were recorded with a UV-Vis detector (λ = 195 nm).

The products recorded, together with their relative retention times, are reported below:

- Glucose (*glc*), t_R = 8,55 min
- Fructose (*fru*), t_R = 9,6 min
- Acetic Acid (*AA*), t_R = 13,1 min
- Levulinic acid (*LA*), t_R = 16,2 min
- 5-Hydroxymethylfurfyral (*5-HMF*), t_R = 33,9 min
- Furfural (*Furf*), t_R = 52,1 min

The retention times of the above mentioned products were acquired both quantitatively and qualitatively by calibration technique with standards at different concentrations, ranging from 50 to 2000 ppm.

Reactivity parameters were calculated as follows:

$$Conversion\ (\%) = \frac{(mmol\ sub\ in) - (mmol\ sub\ out)}{mmol\ sub\ in} \cdot 100$$

$$Carbon\ balance\ (\%) = \frac{\sum_i (mmol\ out) \cdot (C\ atoms)}{(mmol\ sub\ out\ \cdot C\ atoms\ glc)} \cdot 100$$

$$Yield\ (\%) = \frac{mmol\ i\ out}{mmol\ sub\ in} \cdot 100$$

where *i* represents a generical product of reaction.

4. RESULTS AND DISCUSSION

Glucose and fructose conversions into LA consist in a series of reactions usually performed in an aqueous acidic medium. The catalyst choice is thus fundamental.
In this thesis work various Si-Ti systems were formulated and deeply studied.

4.1 Hydrothermal and mechanical stability

SBA-15 is an ordered mesoporous silica which is not stable under the severe hydrothermal conditions required for sugary feedstocks conversion into LA. Moreover, the silica substrate is characterized by a lack of mechanical stability. Due to the above mentioned reasons, the SBA-15 silica matrix has been modified by the introduction of titanium as co-support.
Two direct synthetic approaches have been studied for TiO_2 introduction differing each other for the Ti precursor used: respectively a salt ($TiOCl_2$) and an alkoxide ($Ti(OBu)_4$). Moreover, for each synthetic method, three different molar Ti amounts have been investigated.
First of all, the morphological features of the materials were examined by Nitrogen physisorption technique.
Isotherms regarding both the pristine silica support and the samples synthetized from the salt (%Ti-SBA15 series) are reported in *Figure 19*.

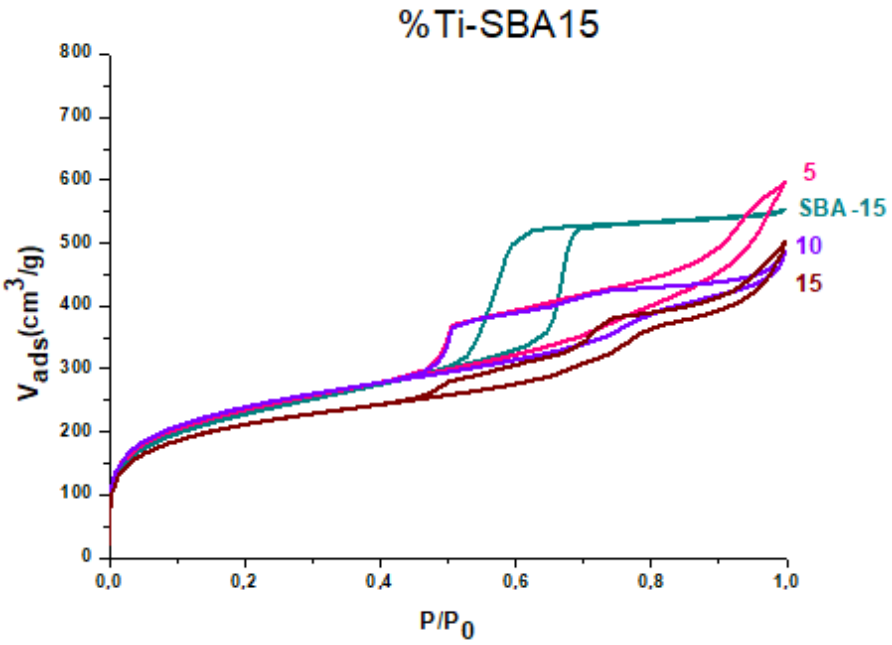

Figure 19: SBA-15 and %Ti-SBA15 physisorption isotherms.

BET surface area (S_{BET}), pore volume and average pore radius values are reported in *Table 1*.

All the samples present Type IV isotherms which are characteristic of mesostructured materials.

The SBA-15 hysteresis is a H1-type, typically associated with porous materials consisting of agglomerates of approximately uniform spheres or well-defined cylindrical-like pore channels. The main difference between the SBA-15 isotherm and the Ti-samples ones consists of the hysteresis shape, indicating that the intrinsic pores' conformation has changed after the Titanium addition. The Si-Ti mixed samples display isotherms more similar to H3-type ones, indicating slit-shaped pores. Moreover, a widening of the hysteresis loops suggests there may be some narrowing of the pore openings following the addition of Ti in the salt form.

The S_{BET} of the samples with 5 and 10 mol.% of Ti respectively, are higher than the one of SBA-15, while the 15-TiSBA15 sample displays a slightly lower area than that of the silica parent material. The S_{BET} decrease in this case may be attributed to a lower amount of Ti (IV) inside the silica network, which may affect the morphological characteristics of the sample.

Samples	**S_{BET}** */$m^2 \cdot g^{-1}$*	***Pores Volume*** */$cm^3 \cdot g^{-1}$*	***Average Pore Dimension*** */nm*
SBA-15	810	0,20	2,5
5Ti-SBA15	845	0,21	2,1
10Ti-SBA15	860	0,21	3,8
15Ti-SBA15	770	0,19	2,1

Table 1: Textural properties of the SBA-15 and %Ti-SBA15 samples.

Isotherms regarding the samples synthetized with the chelating agent (%TiAcAc samples) and parent SBA-15 support are reported in *Figure 20*.

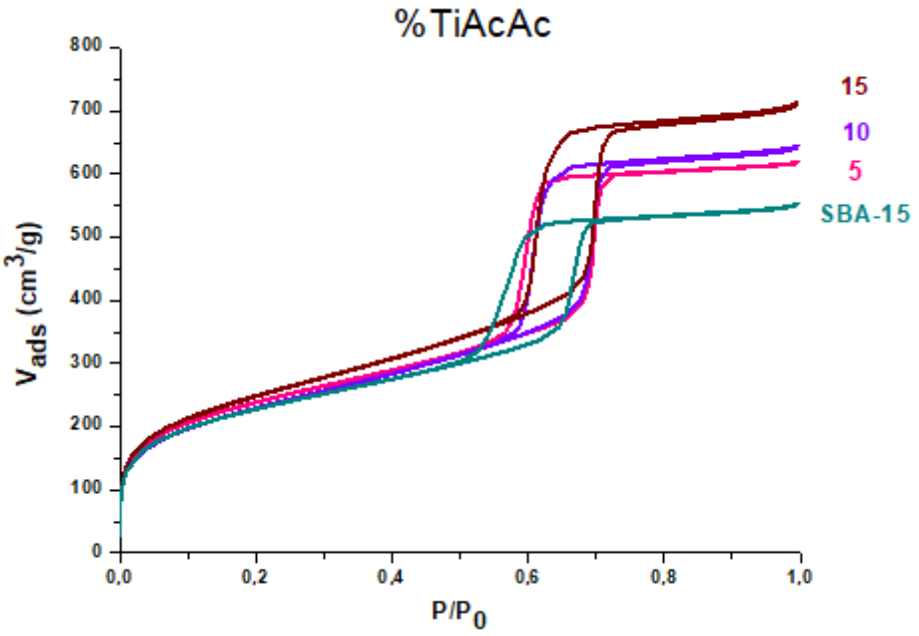

Figure 20: SBA-15 and %TiAcAc physisorption isotherms.

The values of BET surface area (S_{BET}), pore volume and average pore radius are reported in *Table 1*.

As can be seen in *Figure 22*, all the samples show Type IV isotherms, indicating mesostructured materials.

The hysteresis shape of all the %TiAcAc samples is comparable to that of the pure silica support, namely a H1-type. The loop is retained too, indicating that no changes in the pores' conformation took place after the Ti addition. Nonetheless, the S_{BET} values of the %TiAcAc samples are higher than that of the SBA-15 parent sample. Indeed, the increasing amount of Ti entails increasing surface area values.

Samples	**S_{BET}** /m^2·g^{-1}	**Pores Volume** /cm^3·g^{-1}	**Average Pore Dimension** /nm
SBA-15	810	0,20	2,5
5TiAcAc	860	0,21	2,7
10TiAcAc	868	0,20	3,3
15TiAcAc	886	0,21	2,8

Table 2: Textural properties of the SBA-15 and the %Ti-SBA15 samples.

In order to investigate the mechanical stability, the synthesized samples were pressed, crushed and sieved to mash size of 14-18 (1-1.4 mm). The morphological characteristics of the pressed samples were evaluated by N_2 physisorption technique.

The isotherms of the pressed %Ti-SBA15 samples (dot lines) and that of the same pristine supports (continuous lines) are reported in *Figure 21*. Indeed, the figure insert exhibits the SBA-15 physisorption profiles before and after the mechanical stress.

BET surface areas values (S_{BET}) of both the pressed and the not-pressed samples are reported in *Table 3*.

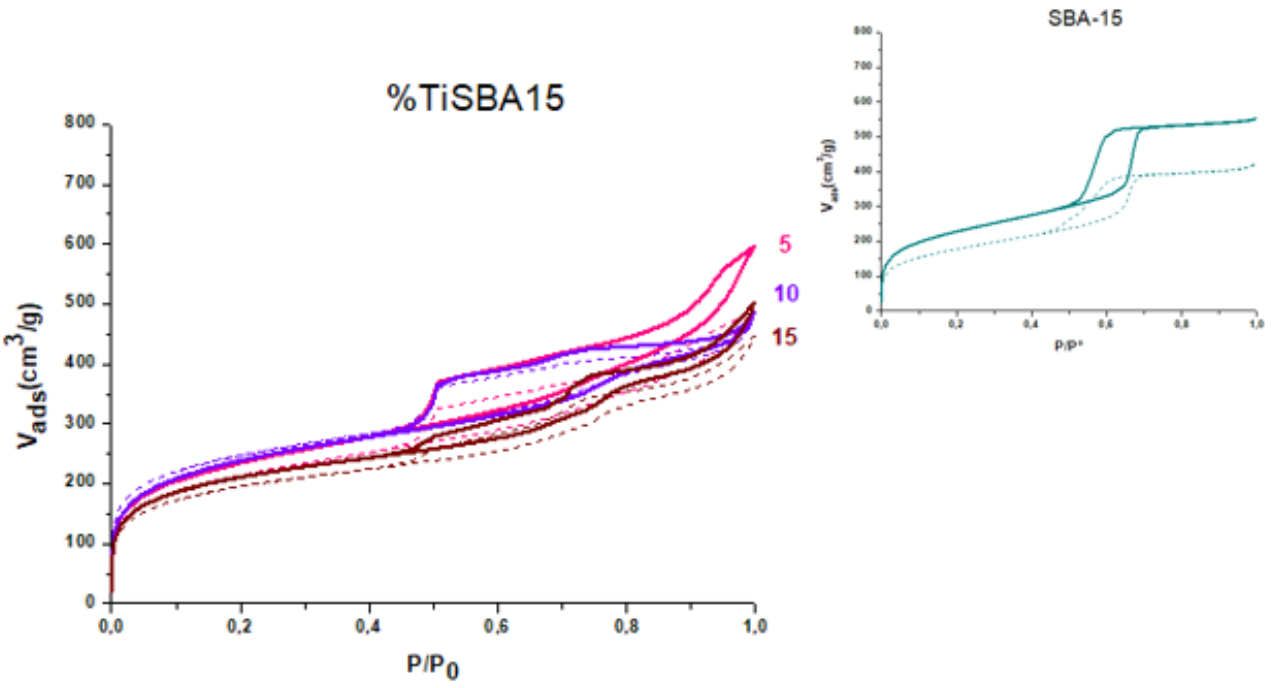

Figure 21: Pressed (dots line) and not-pressed %Ti-SBA15 samples physisorption isotherms; insert: pressed and not-pressed SBA-15 physisorption profiles.

After the test, the SBA-15 isotherm remains a type IV. However, the loop shape hysteresis changes, indicating an alteration of the pores' conformation. A loss of the regular pore arrangement was thus displayed after the mechanical test. This result is confirmed by the remarkable decrease of the S_{BET} value, proving that the SBA-15 is not mechanically stable. For what concerns all the %Ti-SBA15 samples, both the isotherm and the loop shape of the hysteresis are retained after the mechanical test. Moreover, for the %Ti-SBA15 series no significant loss of the S_{BET} values was detected after the mechanical stress. Therefore, the addition of Ti in the salt form seems to have improved the mechanical stability of the samples.

Samples	S_{BET} /$m^2 \cdot g^{-1}$	S_{BET} /$m^2 \cdot g^{-1}$
	Not-pressed sample	***Pressed sample***
SBA-15	810	630
5Ti-SBA15	845	775
10Ti-SBA15	860	860
15Ti-SBA15	770	710

Table 3: S_{BET} of the pressed and not-pressed %Ti-SBA15 samples.

Regarding the %TiAcAc series, the preparation of the supports for the mechanical tests, as reported in the experimental part, was hard to perform, so that only the 5AcAc sample was tested.

The isotherms of both the pressed (dot line) and the not-pressed sample (continuous line) are shown in *Figure 22*.

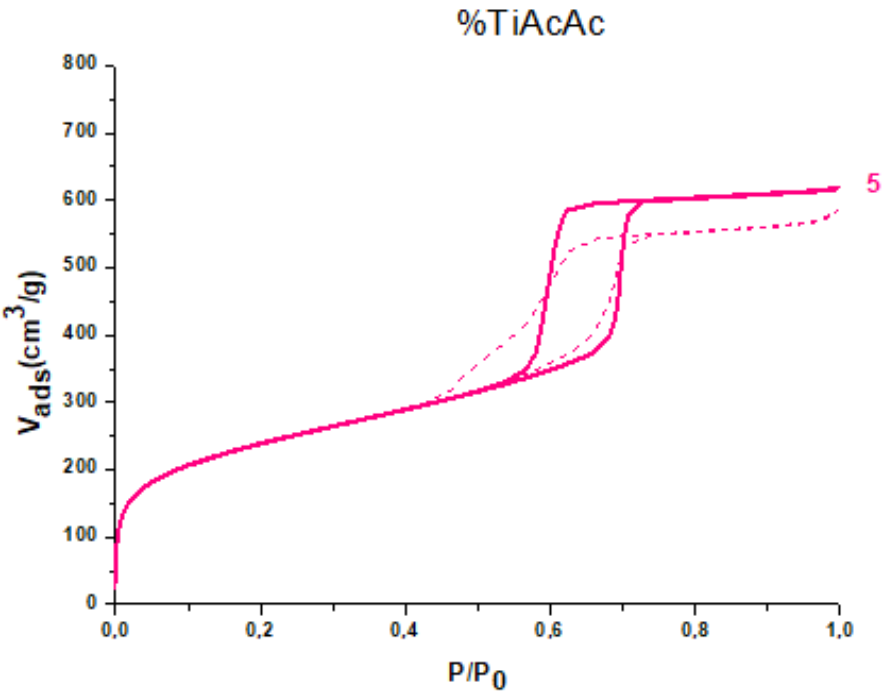

Figure 22: Pressed (dots line) and not-pressed 5TiAcAc sample physisorption isotherms.

It is evident that after the mechanical test the sample retains a type IV isotherm, indicating that the ordered mesostructure is retained. Moreover, the S_{BET} value of the 5AcAc pressed sample is unchanged (860 $m^2 \cdot g^{-1}$) with respect to that of the not pressed one (860 $m^2 \cdot g^{-1}$). However, the hysteresis loop shape is partially altered, disclosing that a slight modification of the pores' conformation occurred. Therefore, it is possible to assert that the Titanium effect over the mechanical stability was less pronounced for the %AcAc series than it was for the %Ti-SBA15 one.

To further understand the structural features of the synthesized materials, XRD analyses were carried out. Samples high angle XRD diffraction patterns are reported in the Appendix. Additionally, Raman analyses were performed at the *University of Turin* and Raman spectra are reported in the Appendix.

Figure 23 displays the low angle XRD diffraction patterns of SBA-15 and the Si-Ti samples synthesized using the Ti salt.

As can be seen, SBA-15 diffraction pattern (*light blue line*) shows three peeks at very low angles (2θ = 0.2°-2°) which correspond to the (100), (110) and the (200) reflection planes, typical of the hexagonal *p6mm* symmetry. However, after the Titanium addition, no well-defined diffraction peeks are detectable in the low angle region, implying that the Si-Ti samples do not display well-ordered structures. Indeed, for all the Si-Ti samples a broad hump indicates a change in the structural properties with respect to the pure silica compound. These results are in agreement with the physisorption analyses.(*Figure 19*)

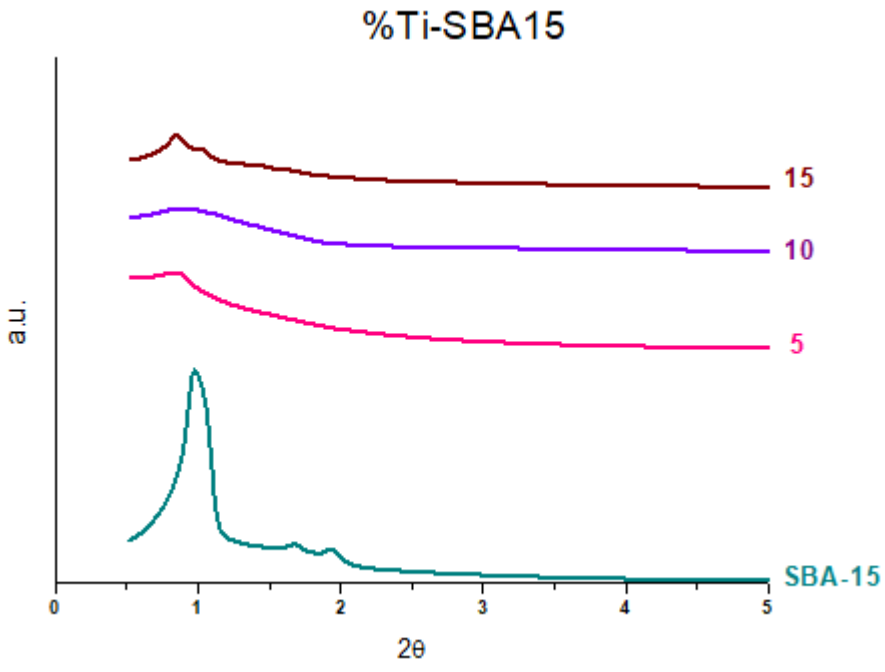

Figure 23: Low angle XRD patterns of SBA-15 and the %Ti-SBA15 samples.

Figure 24 shows the low angle XRD patterns of SBA-15 and that of the Si-Ti samples synthesized using the chelating agent. All the samples prepared with different amounts of Ti showed the typical (100), (110) and (200) diffraction peaks of the 2D-hexagonal *p6mm* structure, typical of SBA-15. Therefore, these materials display highly ordered structures, comparable to the silica parent sample. This result is in line with the N_2-physoisorption analysis reported in *Figure 20,* as also the %TiAcAc isotherms displayed the same profile as that of the pristine material, proving that the SBA-15 ordered structure is retained after the Ti addition.

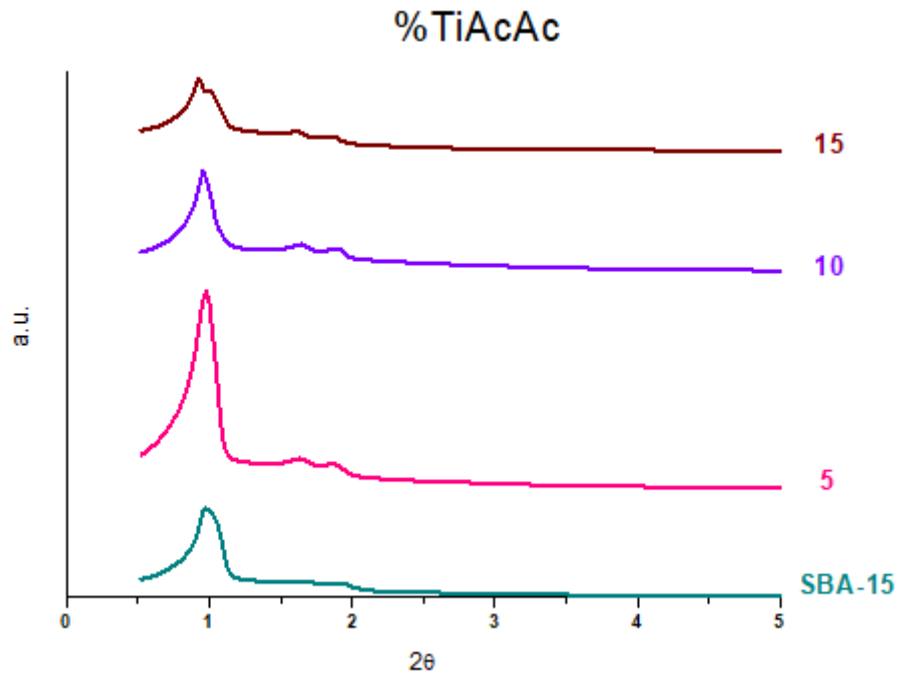

Figure 24: Low angle XRD patterns of SBA-15 and the %TiAcAc samples.

In order to evaluate the hydrothermal stability of the supports, the materials have been evaluated by hydrothermal tests.

The weight amount of the recovered catalyst has been taken into account. However, besides the introduction of titanium, the amount of the solids recovered was very low.

Due to the difficulties encountered during the preparation of the %AcAc samples for the tests, the study has been focused over the Ti salt derived materials. The higher amount was obtained with the 10Ti-SBA15 sample (4 wt.%). Therefore, thanks to its morphological and stability properties, the 10Ti-SBA15 support was selected to further continue the investigation over the material.

According to the literature, in the case of titanium incorporated SBA-15, the amount of tetrahedrally coordinated Ti (IV) species increases with the calcination temperature.[133] Therefore, a further study was performed in order to evaluate different calcination temperatures effect on both the morphological properties and the stability characteristics of the Si-Ti material. The same study was conducted for both the 5Ti-SBA15 and the 15Ti-SBA15 samples. Results are reported in the Appendix.

The temperatures selected for the screening have been 650 °C and 750 °C, which were compared to the 550 °C one.

The isotherms of the not pressed 10Ti-SBA15 samples (continuous lines) and that of the pressed ones (dots lines), referred to a specific temperature of calcination evaluated, are reported in *Figure 25*. The relative values of the S_{BET} are reported in *Table 4.*

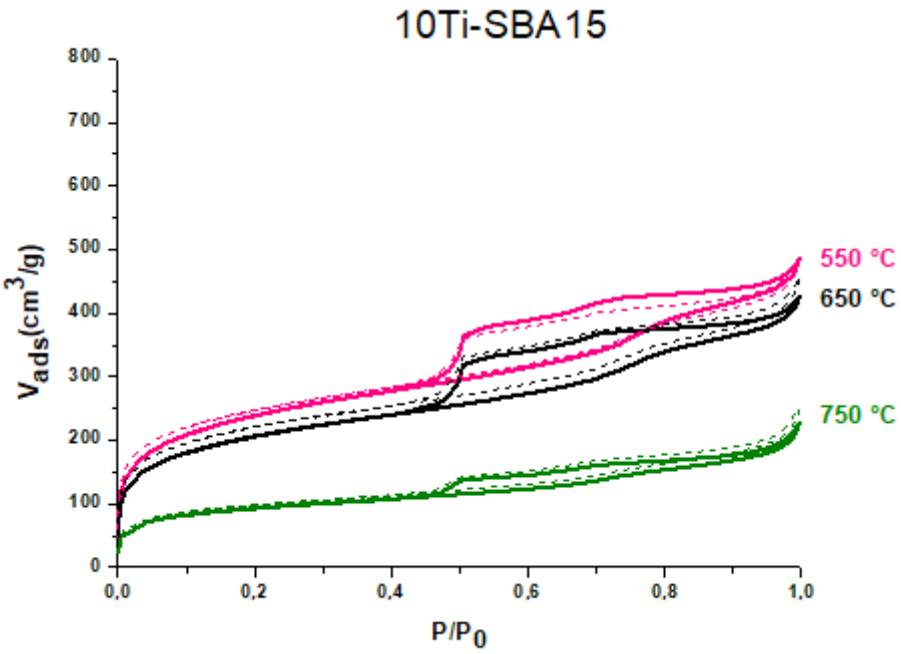

Figure 25: Isotherms of the pressed (dot lines) and not pressed 10Ti-SBA15 samples, calcined at different temperatures.

The Type IV isotherm of the 10Ti-SBA15 support is retained considering the three different temperatures of calcination (550 °C, 650 °C and 750 °C), as well as the hysteresis shape which is in every case a H3-type. As expected, the specific surface area of the material decreases with the increasing temperature of calcination. This effect is more evident in the case of the highest temperature of calcination (750 °C), for which the decrease of the area with respect to the material calcined at 550 °C is of about 500 $m^2 \cdot g^{-1}$. Instead, the area of the support calcined at 650 °C decreases of about 100 $m^2 \cdot g^{-1}$ with respect to the material calcined at 550 °C (*Table 4*).

The mechanical stability is high for all the samples, as no change for both the isotherm and the hysteresis shape is detected after the test. Moreover, no significant loss of surface area occurs (see *Table 4*). Therefore, the support can be defined mechanically stable, also if the temperature of the thermal treatment is increased.

T of calcination /°C	**S_{BET}** /$m^2 \cdot g^{-1}$ ***Not-pressed sample***	**S_{BET}** /$m^2 \cdot g^{-1}$ ***Pressed sample***
550	860	860
650	750	745
750	340	330

Table 4: S_{BET} of the 10Ti-SBA15 pressed and not-pressed samples calcined at different temperature.

Hydrothermal tests were additionally performed over the above mentioned samples.
However, no influence over the stability property has been detected by varying the temperatures of calcination of the samples.
Among all the synthesized supports the sample calcined at 650 °C was selected for further studies because it represents the best compromise between morphological and structural properties, but also due to its stability features as well as sustainability in terms of synthetic approach.

4.2 Acidity

The 10Ti-SBA15 sample calcined at 650 °C, from here labelled TiSB, was selected as catalytic support for further functionalization.
The Brønsted acidity, necessary to carry out the glucose hydrolysis, was given to the Si-Ti matrix via hydrothermal promoted grafting, using a thiol functionalized silica alkoxide,

namely the (3-Mercaptopropyl)trimethoxysilane (MPTMS). The acidic function was obtained after an oxidation treatment. The acid functionalized sample is named TiSB-SO_3H.

In order to evaluate the efficiency of both the grafting process and the oxidation reaction, after each step of the synthesis a TPO analysis was carried out. The results are reported in *Figure 26*. Section *a)* is referred to the grafted support (TiSB-SH), while the *b)* one is referred to the grafted support after the oxidation treatment (TiSB-SO_3H).

From the TiSB-SH analysis two peaks are detectable. The first one, which occurred at temperature <350°C can be attributed to thiol (–SH) or disulfide (–S-S-) decomposition.[134,135] The other peak observed between 400 - 600°C corresponds to the decomposition of the alkyl chain. This result qualitatively highlights the functionalization of the support.

The TPO analysis of the acid substrate (TiSB-SO_3H) reveals no peaks in the range of temperature where the decomposition of the thiol function occurs, thus indicating that the oxidation of the organosulfur compound took place. A peak is present in the range of temperature between 400 - 600°C, indicating the decomposition of both the propyl sulfonic acid groups and the hydrocarbon chains.[136]

Therefore, the TPO analyses showed that the grafting functionalization occurred.

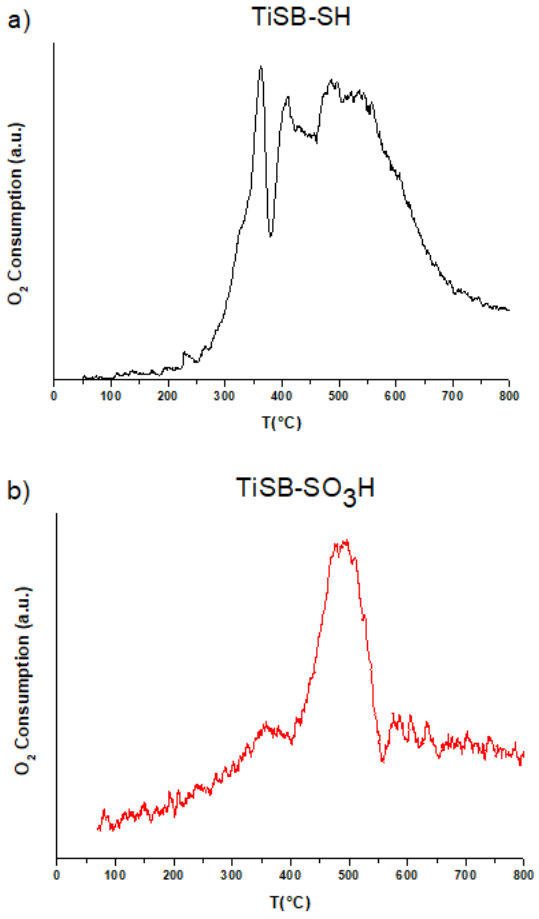

Figure 26: TPO analyses of the TiSB grafted support.

In order to further evaluate the acid property of the functionalized TiSB catalyst, the amount of total Brønted-acid sites was determined by a titration method reported in literature. The value obtained for the TiSB-SO_3H catalyst was qualitatively compared to the one obtained for the SBA-15 system.

The titration results are reported in *Table 5*. The molar values reported are referred to the total amount of Brønsted-acid sites on the catalyst surface.[132]

SBA-15	*TiSB-SO_3H*
$0{,}4 \cdot 10^{-4}$ mol	*$1 \cdot 10^{-4}$ mol*

Table 5: Total Brønted-acid sites calculated via tritration method.[132]

As it is possible to see the total amount of acid sites is higher in the case of the grafted catalyst, confirming the successful functionalization approach.

4.3 Reactivity tests

With the aim of evaluating both the activity and the selectivity of the synthesized catalysts toward LA production, both glucose and fructose hydrolysis reactivity tests were carried out. Reagent conversion, both 5-HMF and LA product yields and the carbon balance values have been taking into account.

First of all, the pristine silica support (SBA-15) and the best mixed Si-Ti system (TiSB) were tested in the aqueous glucose hydrolysis. Their reactivity was further compared to that of the grafted catalyst (TiSB-SO_3H). The reactivity results are reported in *Figure 27*.

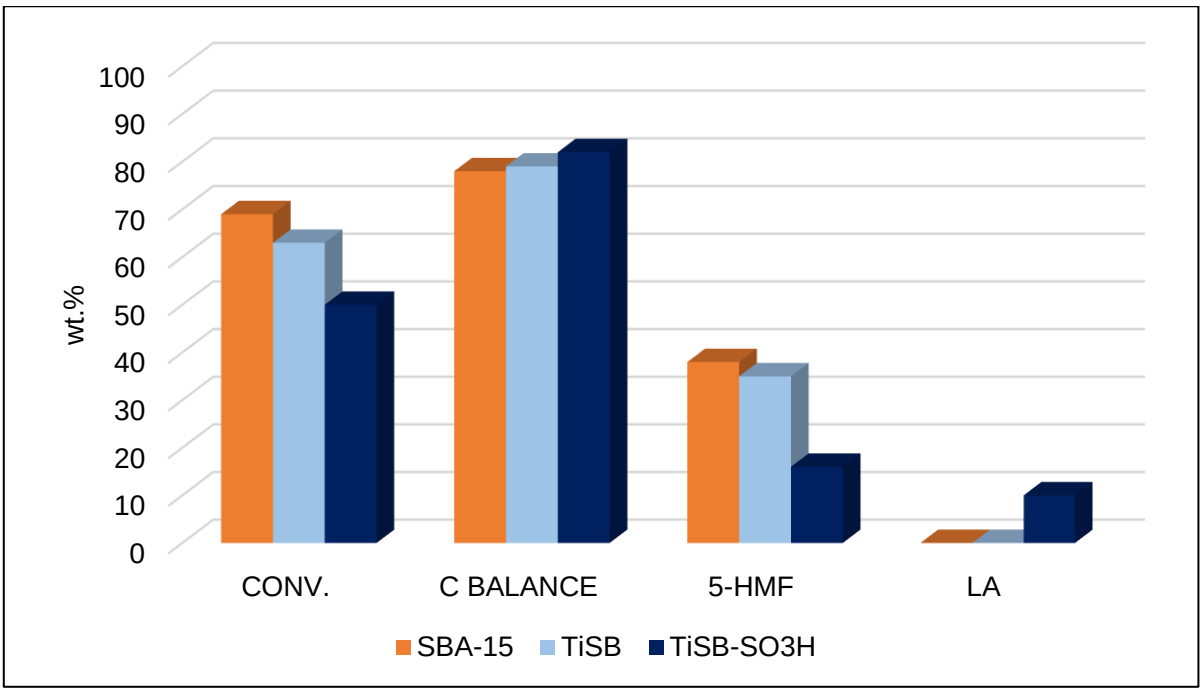

Figure 27: SBA-15, Ti-SB and TiSB-SO_3H reactivity results.

The catalytic performance of the two supports, the silica and the silca-titania one, are comparable. As expected, the absence of Brønsted acidity for both the systems determines no catalytic activity toward the last reaction step, by which LA and an equivalent of formic acid are obtained from the 5-HMF intermediate. Thus, the major reaction product is 5-HMF in both the cases.

Evaluating the activity of the TiSB-SO_3H acid functionalized catalyst the effectiveness of the grafting process can be highlight. As it is possible to see, the TiSB-SO_3H catalyst gives a LA yield of 10wt.%. These results prove that the Brønsted acidity given to the support by the hydrothermal grafting process provides the mixed Si-Ti system with the acid characteristics needed in order to obtain LA. Additionally, the TiSB-SO_3H catalyst, presented a higher carbon balance, thus favouring a lower production of undesired products, such as humins, and acting as a more selective catalyst.

The TiSB-SO_3H catalyst was further tested in the fructose hydrolysis in order to obtain LA. In *Figure 28 t*he catalytic results are compared with that obtained using glucose.

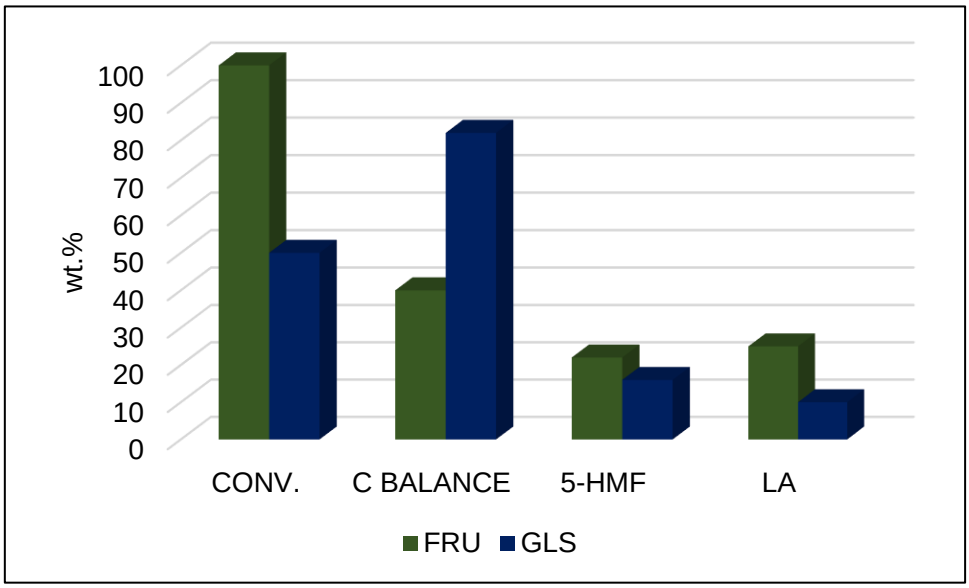

Figure 28: Fructose vs. glucose reactivity test using TiSB-SO_3H as catalyst.

The LA yield using fructose as reactive substrate is higher than that obtained from glucose (25 vs.10 wt.%). Therefore, the glucose isomer acts as a more reactive sugary feedstock, as expected by literature data.[65] The 5-HMF yield obtained with the two different reagents is comparable, particularly it is slightly higher using fructose as reagent (22 vs. 16 wt.%). A conversion of 100 % is detected in the case of fructose, exactly twice the amount of that obtained with glucose. On the other hand, the selectivity in this case is much less, since the carbon balance detected in the fructose hydrolysis was half the one obtained using glucose as sugary feedstock, indicating a high formation of byproducts such as humins.

Additionally, the TiSB-SO_3H catalyst was compared with a traditional acid heterogeneous catalyst, particularly a sulfated zirconia (SZ), prepared via microwave heating. This material is characterized by a good hydrothermal resistance with respect to the silica-titania grafted catalyst. The SZ sample was prepared at the *University of Turin* and it was tested at the *Ca' Foscari University of Venice* thanks to a collaboration. SZ synthetic procedure is described in the Appendix.
The samples were investigated in the glucose hydrolysis and the results are reported in *Figure 29*.

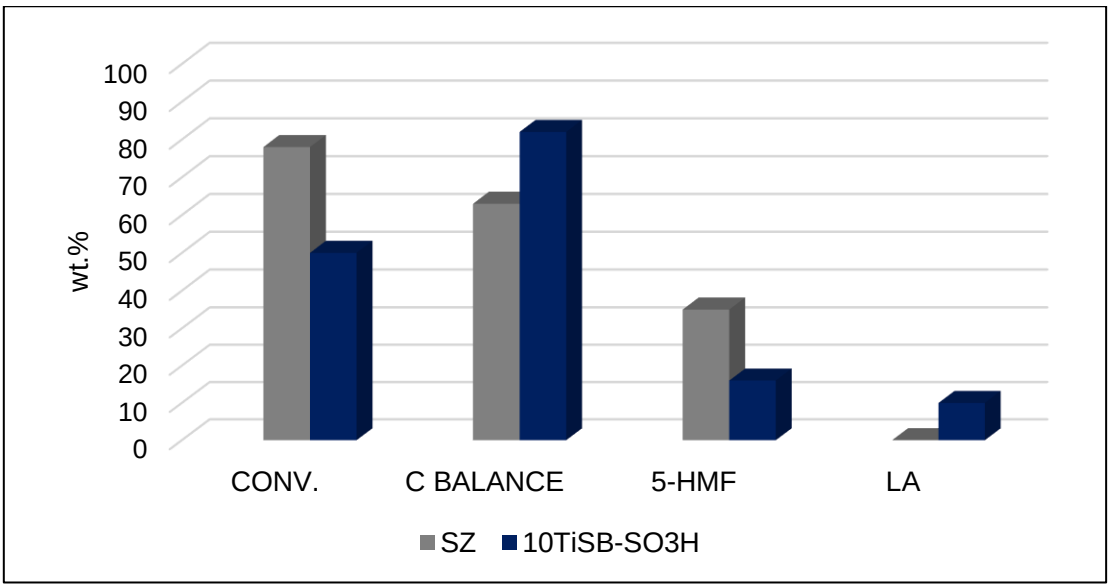

Figure 29: SZ and TiSB-SO_3H glucose hydrolysis tests.

The 5-HMF SZ yield (35 wt.%) was higher than that resulting with the TiSB-SO_3H catalyst (16 wt.%), indicating a major selectivity toward this intermediate than the TiSB-SO_3H has. Nonetheless, the SZ activity stops at this reaction product, because, as occurred with both the Si-Ti support and its silica parent material (see *Figure 27*), no LA was detected. Moreover, in the case of the SZ catalytic system, the glucose conversion was higher than the one obtained with the Si-Ti grafted support (78 vs. 50 wt.%), while the corresponding carbon balance was lower (63 vs. 82 wt.%). This points out a resulting higher production of undesirable and irreversible byproducts, such as humins, in the presence of the SZ catalyst. The two different catalytic behaviors are probably the result of several factors, such as morphological and structural differences between the two systems. The SZ's surface area (35 $m^2 \cdot g^{-1}$), for example, is highly lower than that of the high surface area Si-Ti material. This feature may negatively affect the SZ catalytic performance as the interactions between the substrate and the surface active sites of the catalyst are drastically reduced. Moreover, the acid active functionalities on the SZ catalyst may not be enough to obtain LA.

The above mention results confirm that the glucose hydrolysis requires catalytic systems with both great acidity and high surface area.

Therefore, the comparison between the TiSB-SO_3H catalyst and another heterogeneous catalyst (SZ), seems indicate that the developed acid functionalized Si-Ti catalyst acts as a promising catalytic system for the obtainment of LA from the glucose hydrolysis.

5. CONCLUSION

Heterogeneous catalysis is a promising alternative to common homogeneous catalysts applied in the field of biomass conversion into chemicals.

In this thesis work, an effective and sustainable synthetic approach for the synthesis of novel Si-Ti heterogeneous catalysts has been developed. The catalytic activity of the best system has been evaluated in the glucose and fructose hydrolysis for LA production.

SBA-15 type Ordered Mesoporous Silica (OMS) has been taken as benchmark due to its attractive properties of high specific surface area and large pores dimentions, necessaries for the catalyst up-scale improvement towards reactions of biomass derived bulky molecules. However, the pristine silica system displays some drawbacks for the desired application. Therefore, deep modifications of the SBA-15 material has been performed, concerning both its stability properties and its acidity aspect.

Hydrothermal and mechanical stability improvements have been achieved tailoring the silica matrix with titania as co-support. In this way two different synthetic approaches were studied, and different tests and characterizations were performed over the Si-Ti composities in order to evaluate the properties of the novel materials. Both the synthetic methods employed have brought promising results with respect to the pristine material.

Concerning the acidity aspect, the best synthesized silica-titania support has been further functionalized with strong acid functionalities required for the glucose hydrolysis. In this way a sustainable synthetic approach was applied since a post grafting technique using an aqueous solution of NaCl as solvent was performed. The activity and the selectivity of the acid catalyst toward LA were evaluated in aqueous batch conditions, confirming that the synthesis of an active catalyst occurred. Moreover, comparing the catalytic activity of the novel catalyst with that of another common acid heterogeneous system, it is possible to assure that the LA yield obtained is a promising result. However, even if the results are encouraging, much effort is still needed in order to obtain a more efficient catalyst. Future efforts could be applied tuning the catalyst design, particularly other amount of Ti can be evaluated in order to optimize the system.

Concluding, even if further development is needed for the obtainment of more satisfying results, promising bases for the formulation of an efficient and robust catalytic system have been achieved.

6. APPENDIX

Mechanical stability tests

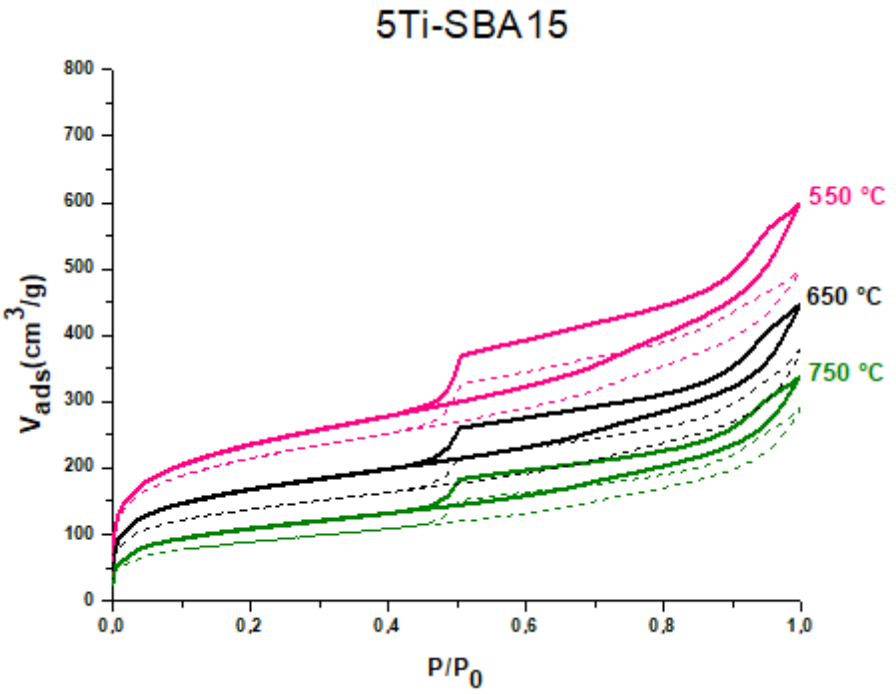

Figure 30: Isotherms of the pressed (dot lines) and not pressed 5Ti-SBA15 samples, calcined at different temperatures.

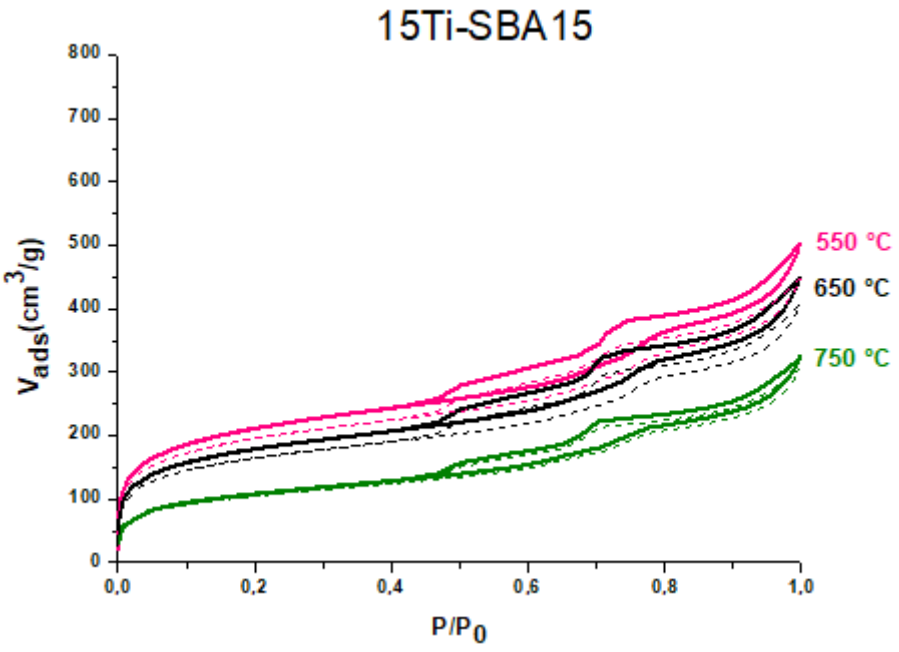

Figure 31: Isotherms of the pressed (dot lines) and not pressed 15Ti-SBA15 samples, calcined at different temperatures.

High angle XRD patterns

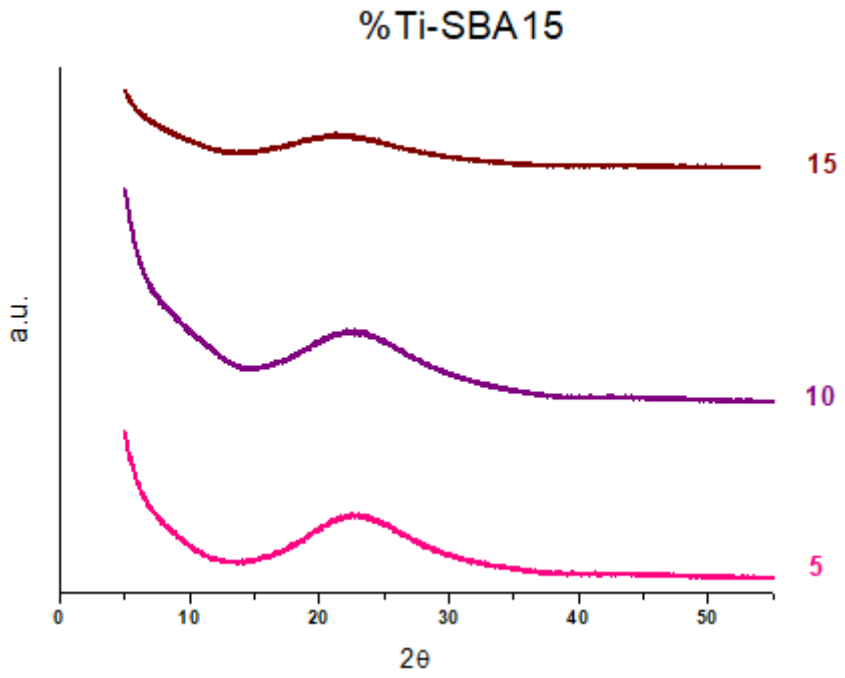

Figure 32: High angle XRD patterns of the %Ti-SBA15 samples.

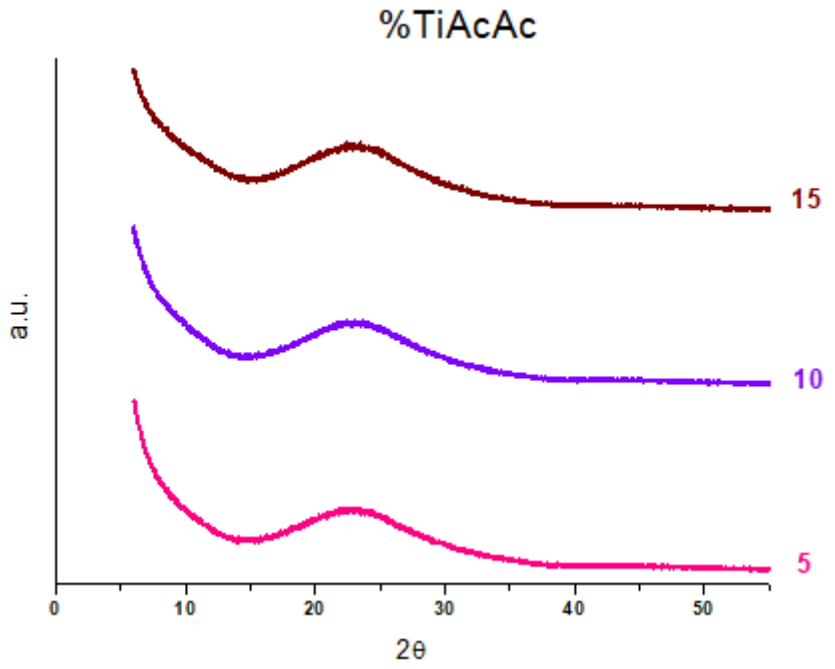

Figure 33: High angle XRD patterns of the %TiAcAc samples.

Raman analyses

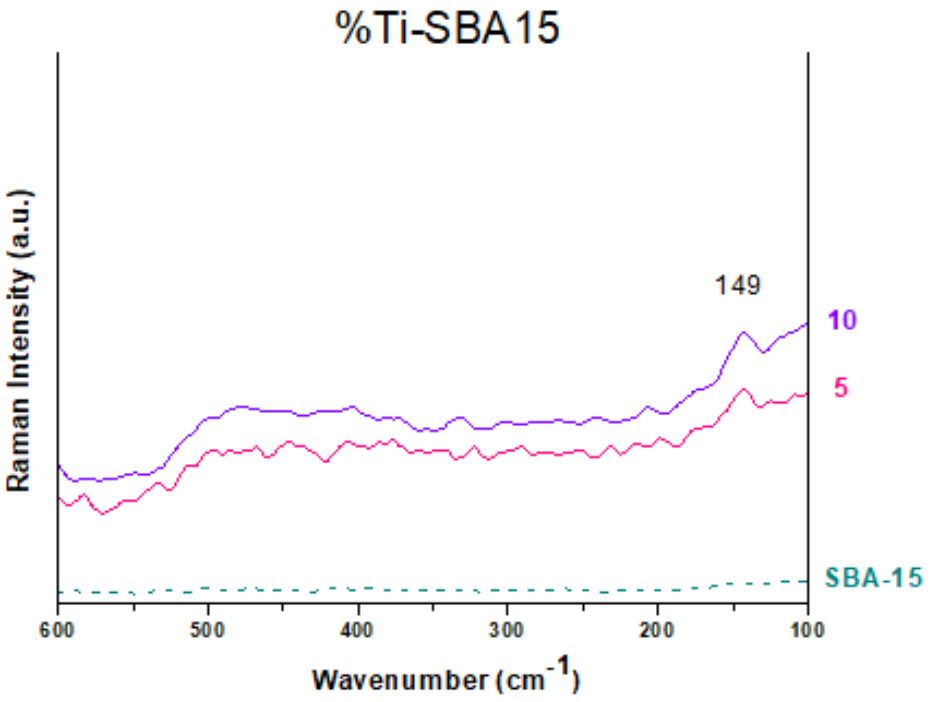

Figure 34: SBA-15, 5Ti-SBA15 and 10Ti-SBA15 Raman spectra.

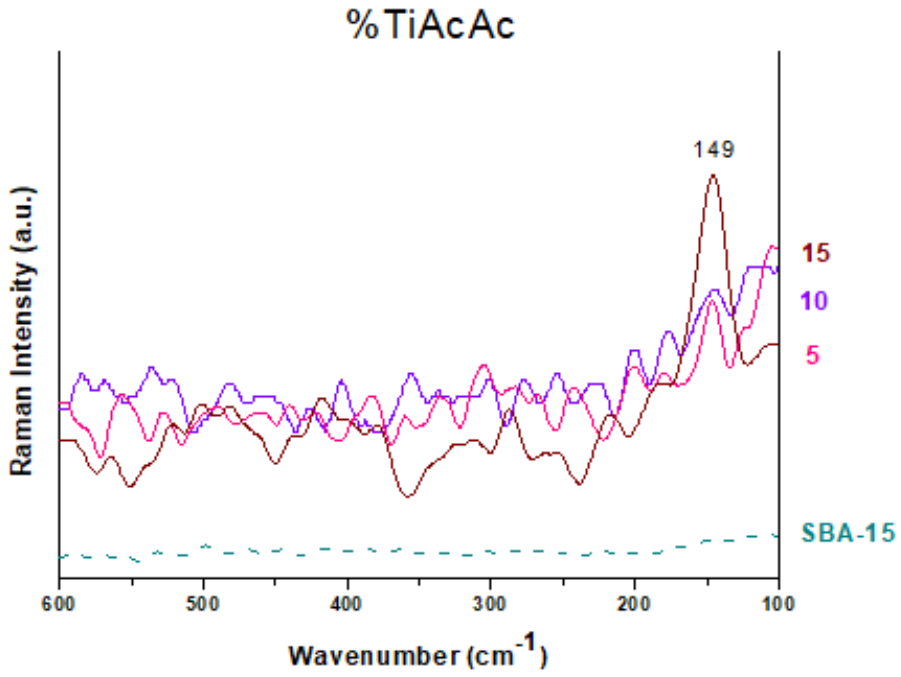

Figure 35: SBA-15, 5TiAcAc, 10TiAcAc and 15TiAcAc Raman spectra.

Sulfated Zirconia synthesis

Zirconia nanoparticles were prepared by a two-step synthetic route, both assisted by microwave heating systems using adapted household microwave oven (SAMSUNG C109STF). To a Zr propoxide solution (70 wt.% in 1-propanol) in ethanol, nitric acid was added to catalyze hydrolysis. Under stirring water was added dropwise until gel formation. The gel obtained was dried in a multimodal microwave oven with cycles at different power until no solvent was collected. The xerogel (X) was washed with ethanol to remove the excess of reagents. The subsequent thermal treatment on the obtained system was carried on in microwave oven using 10 g of graphite as susceptor.[137] Sulfates were added by wetness impregnation (WI) with a 0,5 M solution of $(NH_4)_2SO_4$ on t-ZrO_2. Thermal treatment in MW oven with graphite as susceptor was carried on samples after impregnation.

7. REFERENCES

[1] X. Li, L. Luque-Moreno, S. Oudenhoven, L. Rehmann, S. Kersten, B. Schuur. “Aromatics Extraction from Pyrolytic Sugars Using Ionic Liquid to Enhance Sugar Fermentability.” *Bioresource Technology*, vol. 216, **2016**, pp. 12–18., doi:10.1016/j.biortech.2016.05.035.

[2] BP Energy Outlook, 2018 Edition. [Online]. Available: https://www.bp.com/content/dam/bp/en/corporate/pdf/energy-economics/energy-outlook/bp-energy-outlook-2018.pdf [Accessed January 2019]

[3] eia *Independent Statistics & Analysis* U.S. Energy Information Administration. [Online]. Available: https://www.eia.gov/. [Accessed February 2019]

[4] M. Bothe. “The Kyoto Protocol As a Pioneer Among the Multilateral Environmental Agreements.” *The Kyoto Protocol and Beyond*, **2007**, pp. 241–246., doi:10.1007/978-90-6704-547-6_18.

[5] J. Rogelj, J. Nabel, C. Chen, W. Hare, K. Markmann, M. Meinshausen, M. Schaeffer, K. Macey, N. Höhne. “Copenhagen Accord Pledges Are Paltry.” *Nature*, vol. 464, no. 7292, **2010**, pp. 1126–1128., doi:10.1038/4641126a.

[6] K. Fløttum, H. Drange. “The Paris COP21 Agreement—Obligations for 195 Countries.” *The Role of Language in the Climate Change Debate*, **2017**, pp. 130–148., doi:10.4324/9781315456935-8.

[7] iea International Energy Agency, [Online]. Available: https://www.iea.org/newsroom/news/2018/october/modern-bioenergy-leads-the-growth-of-all-renewables-to-2023-according-to-latest-.html. [Accessed December 2018].

[8] iea International Energy Agency, “Renewables 2018 Market analysis and forecast from 2018 to 2023” [Online]. Available: https://www.iea.org/renewables2018/. [Accessed December 2018].

[9] European Commission [Online]. Available: https://ec.europa.eu/research/bioeconomy/pdf/review_of_2012_eu_bes.pdf [Accessed January 2019].

[10] EUR-Lex Access to European Union law [Online]. Available: https://ec.europa.eu/programmes/horizon2020/en/h2020-section/secure-clean-and-efficient-energy. [Accessed January 2019].

[11] European Commission [Online]. Available: https://eur-lex.europa.eu/legal-content/EN/ALL/?uri=celex%3A32009L0028. [Accessed December 2018].

[12] L. Granone, F. Sieland, N. Zheng, R. Dillert, D. Bahnemann. “Photocatalytic Conversion of Biomass into Valuable Products: a Meaningful Approach?” *Green Chemistry*, vol. 20, no. 6, **2018**, pp. 1169–1192., doi:10.1039/c7gc03522e.

[13] U. Corato, I. Bari, E. Viola, M. Pugliese. “Assessing the Main Opportunities of Integrated Biorefining from Agro-Bioenergy Co/by-Products and Agroindustrial Residues into High-Value Added Products Associated to Some Emerging Markets: A Review.” *Renewable and Sustainable Energy Reviews*, vol. 88, **2018**, pp. 326–346., doi:10.1016/j.rser.2018.02.041.

[14] C.B. Field. “Primary Production of the Biosphere: Integrating Terrestrial and Oceanic Components.” *Science*, vol. 281, no. 5374, **1998**, pp. 237–240., doi:10.1126/science.281.5374.237.

[15] P. J., Dunn. “The Importance of Green Chemistry in Process Research and Development.” *Chem. Soc. Rev.*, vol. 41, no. 4, **2012**, pp. 1452–1461., doi:10.1039/c1cs15041c.

[16] X. Zhang, K. Wilson, A. Lee. “Heterogeneously Catalyzed Hydrothermal Processing of C5–C6 Sugars.” *Chemical Reviews*, vol. 116, no. 19, **2016**, pp. 12328–12368., doi:10.1021/acs.chemrev.6b00311.

[17] L. Petrus, M.A. Noordermeer. “Biomass to Biofuels, a Chemical Perspective.” *Green Chemistry*, vol. 8, no. 10, **2006**, p. 861., doi:10.1039/b605036k.

[18] R.A. Sheldon. “Green and Sustainable Manufacture of Chemicals from Biomass: State of the Art.” *Green Chem.*, vol. 16, no. 3, **2014**, pp. 950–963., doi:10.1039/c3gc41935e.

[19] S. Tabasso, D. Carnaroglio, E. Gaudino, G. Cravotto. “ChemInform Abstract: Microwave, Ultrasound and Ball Mill Procedures for Bio-Waste Valorisation.” *ChemInform*, vol. 46, no. 16, **2015**, doi:10.1002/chin.201516335.

[20] M. Nadia, V. Castellani, S. Sala. “Current Options for the Valorization of Food Manufacturing Waste: a Review.” *Journal of Cleaner Production*, vol. 65, **2014**, pp. 28–41., doi:10.1016/j.jclepro.2013.10.051.

[21] H. Vogel. “Catalysis for Renewables. From Feedstock to Energy Production. Edited by Gabriele Centi and Rutger A. Van Santen.” *ChemSusChem*, vol. 1, no. 3, **2008**, pp. 262–262., doi:10.1002/cssc.200700153.

[22] European Environmental Agency Report [Online]. Available: https://www.eea.europa.eu/publications/eea_report_2006_7/file [Accessed January 2019]

[23] J. Bozell. “Feedstocks for the Future: Using Technology Development as a Guide to Product Identification.” *ACS Symposium Series Feedstocks for the Future*, **2006**, pp. 1–12., doi:10.1021/bk-2006-0921.ch001.

[24] E. Kunkes, D. Simonetti, R. West, J. Serrano-Ruiz, C. Gartner, J. Dumesic. “Catalytic Conversion of Biomass to Monofunctional Hydrocarbons and Targeted Liquid-Fuel Classes.” *Science*, vol. 322, no. 5900, **2008**, pp. 417–421., doi:10.1126/science.1159210.

[25] Z. Miao, T. Grift, A. Hansen, K. Ting. “An Overview of Lignocellulosic Biomass Feedstock Harvest, Processing and Supply for Biofuel Production.” *Biofuels*, vol. 4, no. 1, **2013**, pp. 5–8., doi:10.4155/bfs.12.76.

[26] M. Taherzadeh, K. Karimi. “Pretreatment of Lignocellulosic Wastes to Improve Ethanol and Biogas Production: A Review.” *International Journal of Molecular Sciences*, vol. 9, no. 9, **2008**, pp. 1621–1651., doi:10.3390/ijms9091621.

[27] S. Behera, R. Arora, N. Nandhagopal, S. Kumar. “Importance of Chemical Pretreatment for Bioconversion of Lignocellulosic Biomass.” *Renewable and Sustainable Energy Reviews*, vol. 36, **2014**, pp. 91–106., doi:10.1016/j.rser.2014.04.047.

[28] P. Mckendry. “Energy Production from Biomass (Part 2): Conversion Technologies.” *Bioresource Technology*, vol. 83, no. 1, **2002**, pp. 47–54., doi:10.1016/s0960-8524(01)00119-5.

[29] H. Ruiz, R. Rodríguez-Jasso, B. Fernandes, A. Vicente, J. Teixeira. “Hydrothermal Processing, as an Alternative for Upgrading Agriculture Residues and Marine Biomass According to the Biorefinery Concept: A Review.” *Renewable and Sustainable Energy Reviews*, vol. 21, **2013**, pp. 35–51., doi:10.1016/j.rser.2012.11.069.

[30] Y. Guo, S.Z. Wang, D.H. Xu, Y.M. Gong, H.H. Ma, X.Y. Tang. “Review of Catalytic Supercritical Water Gasification for Hydrogen Production from Biomass.” *Renewable and Sustainable Energy Reviews*, vol. 14, no. 1, **2010**, pp. 334–343., doi:10.1016/j.rser.2009.08.012.

[31] A.J. Ragauskas, C.K. Williams, B.H. Davison, G. Britovsek, J. Cairney, C.A. Eckert, W.J. Frederick Jr., J.P. Hallett, D.J. Leak, C.L. Liotta, J.R. Mielenz, R. Murphy, R. Templer, T. Tschaplinski. “The Path Forward for Biofuels and Biomaterials.” *Science*, vol. 311, no. 5760, **2006**, pp. 484–489., doi:10.1126/science.1114736.

[32] S. Vassilev, D. Baxter, L. Andersen, C. Vassileva. “An Overview of the Chemical Composition of Biomass.” *Fuel*, vol. 89, no. 5, 2010, pp. 913–933., doi:10.1016/j.fuel.2009.10.022.

[33] T. Werpy, G. Petersen. “Top Value Added Chemicals from Biomass: Volume I -- Results of Screening for Potential Candidates from Sugars and Synthesis Gas.” **2004**, doi:10.2172/15008859.

[34] P. Zhou, Z. Zhang. “One-Pot Catalytic Conversion of Carbohydrates into Furfural and 5-Hydroxymethylfurfural.” *Catalysis Science & Technology*, vol. 6, no. 11, **2016**, pp. 3694–3712., doi:10.1039/c6cy00384b.

[35] S. Wang, G. Dai, H. Yang, Z. Luo. “Lignocellulosic Biomass Pyrolysis Mechanism: A State-of-the-Art Review.” *Progress in Energy and Combustion Science*, vol. 62, **2017**, pp. 33–86., doi:10.1016/j.pecs.2017.05.004.

[36] J. Wang, B. Shen, D. Kang, P. Yuan, C. Wu. “Investigate the Interactions between Biomass Components during Pyrolysis Using in-Situ DRIFTS and TGA.” *Chemical Engineering Science*, vol. 195, **2019**, pp. 767–776., doi:10.1016/j.ces.2018.10.023.

[37] L. Mika, E. Cséfalvay, Á. Németh. “Catalytic Conversion of Carbohydrates to Initial Platform Chemicals: Chemistry and Sustainability.” *Chemical Reviews*, vol. 118, no. 2, **2017**, pp. 505–613., doi:10.1021/acs.chemrev.7b00395.

[38] D. Alonso, S. Wettstein, J. Dumesic. “Bimetallic Catalysts for Upgrading of Biomass to Fuels and Chemicals.” *Chemical Society Reviews*, vol. 41, no. 24, **2012**, p. 8075., doi:10.1039/c2cs35188a.

[39] D. Roy, M. Semsarilar, J. Guthrie, S. Perrier. “Cellulose Modification by Polymer Grafting: a Review.” *Chemical Society Reviews*, vol. 38, no. 7, 2009, p. 2046., doi:10.1039/b808639g.

[40] D. Alonso, S. Wettstein, J. Dumesic. “Gamma-Valerolactone, a Sustainable Platform Molecule Derived from Lignocellulosic Biomass.” *Green Chemistry*, vol. 15, no. 3, **2013**, p. 584., doi:10.1039/c3gc37065h.

[41] C. Zhou, X. Xia, C. Lin, D. Tong, J. Beltramini. “Catalytic Conversion of Lignocellulosic Biomass to Fine Chemicals and Fuels.” *Chemical Society Reviews*, vol. 40, no. 11, **2011**, p. 5588., doi:10.1039/c1cs15124j.

[42] Z. Strassberger, S. Tanase. “The Pros and Cons of Lignin Valorisation in an Integrated Biorefinery.” *RSC Adv.*, vol. 4, no. 48, **2014**, pp. 25310–25318., doi:10.1039/c4ra04747h.

[43] M. Aresta, A. Dibenedetto. “Catalysis for the Valorization of Low-Value C-Streams.” *Journal of the Brazilian Chemical Society*, **2014**, doi:10.5935/0103-5053.20140257.

[44] P. Gullón, A. Romaní, C. Vila, G. Garrote, J.C. Parajó. “Biofuels, Bioproducts and Biorefining.” vol. 6, no. 2, **2012**, pp. 219–232., doi:10.1002/bbb.v6.2.

[45] R. Weingarten, Y. Kim, G. Tompsett, A. Fernández, K. Han, E. Hagaman, W. Conner, J. Dumesic, G. Huber “Conversion of Glucose into Levulinic Acid with Solid Metal(IV) Phosphate Catalysts.” *Journal of Catalysis*, vol. 304, **2013**, pp. 123–134., doi:10.1016/j.jcat.2013.03.023.

[46] Web of Science (key word Levulinic acid) [Online]. Available: https://apps.webofknowledge.com/WOS_GeneralSearch_input.do?product=WOS&search_mode=GeneralSearch&SID=F1FCAnYGdJUc2LbgqnO&preferencesSaved= [Accessed February 2019]

[47] D.W. Rackemann, W.O.S. Doherty. “The Conversion of Lignocellulosics to Levulinic Acid.” *Biofuels, Bioproducts and Biorefining*, vol. 5, no. 2, **2011**, pp. 198–214., doi:10.1002/bbb.267.

[48] Grand View Research. Levulinic acid market to grow at 5.7% CAGR from 2014 to 2020. [Online]. Available: http://www.grandviewresearch.com/pressrelease/global-levulinic-acid-market. [Accessed January 2019].

[49] M.J. Climent, A. Corma, S. Iborra. “Conversion of Biomass Platform Molecules into Fuel Additives and Liquid Hydrocarbon Fuels.” *Green Chemistry*, vol. 16, no. 2, **2014**, p. 516., doi:10.1039/c3gc41492b.

[50] J. Bozell, L. Moens, D.C. Elliott, Y. Wang, G.G. Neuenscwander, S.W. Fitzpatrick, R.J. Bilski, J.L. Jarnefeld. “Production of Levulinic Acid and Use as a Platform Chemical for Derived Products.” *Resources, Conservation and Recycling*, vol. 28, no. 3-4, **2000**, pp. 227–239., doi:10.1016/s0921-3449(99)00047-6.

[51] L.E. Manzer. “Biomass Derivatives: A Sustainable Source of Chemicals.” *ACS Symposium Series Feedstocks for the Future*, **2006**, pp. 40–51., doi:10.1021/bk-2006-0921.ch004.

[52] D.J. Braden, C.A. Henao, J. Heltzel, C.C. Maravelias, J.A. Dumesic. “Production of Liquid Hydrocarbon Fuels by Catalytic Conversion of Biomass-Derived Levulinic Acid.” *Green Chemistry*, vol. 13, no. 7, **2011**, pp. 1755–1765., doi:10.1039/c1gc15047b.

[53] I.T. Horváth, H. Mehdi, V. Fábos, L. Boda, L.T. Mika. “γ-Valerolactone—a Sustainable Liquid for Energy and Carbon-Based Chemicals.” *Green Chem.*, vol. 10, no. 2, **2008**, pp. 238–242., doi:10.1039/b712863k.

[54] J.-P. Lange, R. Price, P.M. Ayoub, J.N. Louis, L. Petrus, L. Clarke, H. Gosselink.“Valeric Biofuels: A Platform of Cellulosic Transportation Fuels.” *Angewandte Chemie International Edition*, vol. 49, no. 26, **2010**, pp. 4479–4483., doi:10.1002/anie.201000655.

[55] J. Bond, D. Alonso, D. Wang, R. West, J. Dumesic. “Integrated Catalytic Conversion of -Valerolactone to Liquid Alkenes for Transportation Fuels.” *Science*, vol. 327, no. 5969, **2010**, pp. 1110–1114., doi:10.1126/science.1184362.

[56] A.S. Amarasekara, S.A. Hawkins. “Synthesis of Levulinic Acid–Glycerol Ketal–Ester Oligomers and Structural Characterization Using NMR Spectroscopy.” *European Polymer Journal*, vol. 47, no. 12, **2011**, pp. 2451–2457., doi:10.1016/j.eurpolymj.2011.09.007.

[57] Y. Guo, K. Li, X. Yu, J. Clark. “Mesoporous $H_3PW_{12}O_{40}$-Silica Composite: Efficient and Reusable Solid Acid Catalyst for the Synthesis of Diphenolic Acid from Levulinic Acid.” *Applied Catalysis B: Environmental*, vol. 81, no. 3-4, **2008**, pp. 182–191., doi:10.1016/j.apcatb.2007.12.020.

[58] S. Chen, T. Maneerung, D. Tsang, Y. Ok, C. Wang. “Valorization of Biomass to Hydroxymethylfurfural, Levulinic Acid, and Fatty Acid Methyl Ester by Heterogeneous Catalysts.” *Chemical Engineering Journal*, vol. 328, **2017**, pp. 246–273., doi:10.1016/j.cej.2017.07.020.

[59] A. Corma, S. Iborra, A. Velty. “Chemical Routes for the Transformation of Biomass into Chemicals.” *ChemInform*, vol. 38, no. 36, **2007**, doi:10.1002/chin.200736263.

[60] J.J. Bozell, G. R. Petersen. “Technology Development for the Production of Biobased Products from Biorefinery Carbohydrates—the US Department of Energy’s ‘Top 10’ Revisited.” *Green Chemistry*, vol. 12, no. 4, **2010**, p. 539., doi:10.1039/b922014c.

[61] M. Musolino, J. Andraos, F. Aricò. “An Easy Scalable Approach to HMF Employing DMC as Reaction Media: Reaction Optimization and Comparative Environmental Assessment.” *ChemistrySelect*, vol. 3, no. 8, **2018**, pp. 2359–2365., doi:10.1002/slct.201800198.

[62] A. Pedersen, R. Ringborg, T. Grotkjær, S. Pedersen, J. Woodley. “Synthesis of 5-Hydroxymethylfurfural (HMF) by Acid Catalyzed Dehydration of Glucose–Fructose Mixtures.” *Chemical Engineering Journal*, vol. 273, **2015**, pp. 455–464., doi:10.1016/j.cej.2015.03.094.

[63] R. Weingarten, J. Cho, R. Xing, W. Conner, G. Huber. “Kinetics and Reaction Engineering of Levulinic Acid Production from Aqueous Glucose Solutions.” *ChemSusChem*, vol. 5, no. 7, **2012**, pp. 1280–1290., doi:10.1002/cssc.201100717.

[64] B. Girisuta, L.P.B.M. Janssen, H.J. Heeres. “Green Chemicals.” *Chemical Engineering Research and Design*, vol. 84, no. 5, **2006**, pp. 339–349., doi:10.1205/cherd05038.

[65] S. Saravanamurugan, M. Paniagua, J. Melero, A. Riisager. “Efficient Isomerization of Glucose to Fructose over Zeolites in Consecutive Reactions in Alcohol and Aqueous Media.” *Journal of the American Chemical Society*, vol. 135, no. 14, **2013**, pp. 5246–5249., doi:10.1021/ja400097f.

[66] M.D. Sweeney, F. Xu. “Biomass Converting Enzymes as Industrial Biocatalysts for Fuels and Chemicals: Recent Developments.” *Catalysts*, vol. 2, no. 2, **2012**, pp. 244–263., doi:10.3390/catal2020244.

[67] Y. Román-Leshkov, M. Moliner, J. Labinger, M. Davis. “Mechanism of Glucose Isomerization Using a Solid Lewis Acid Catalyst in Water.” *Angewandte Chemie International Edition*, vol. 49, no. 47, **2010**, pp. 8954–8957., doi:10.1002/anie.201004689.

[68] Y.B. Tewari, R.N. Goldberg. “Thermodynamics of the Conversion of Aqueous Glucose to Fructose.” *Applied Biochemistry and Biotechnology*, vol. 11, no. 1, **1985**, pp. 17–24., doi:10.1007/bf02824308.

[69] F. Menegazzo, E. Ghedini, M. Signoretto. “5-Hydroxymethylfurfural (HMF) Production from Real Biomasses.” *Molecules*, vol. 23, no. 9, **2018**, p. 2201., doi:10.3390/molecules23092201.

[70] R.-J. Putten, J.C. Waal, E. Jong, C.B. Rasrendra, H.J. Heeres, J.G. Vries. “Hydroxymethylfurfural, A Versatile Platform Chemical Made from Renewable Resources.” *Chemical Reviews*, vol. 113, no. 3, **2013**, pp. 1499–1597., doi:10.1021/cr300182k.

[71] J. Serrano-Ruiz, J. Dumesic. “Catalytic Routes for the Conversion of Biomass Into Liquid Hydrocarbon Transportation Fuels.” *Advanced Biofuels*, **2015**, pp. 115–156., doi:10.1201/b18526-7.

[72] E. Gürbüz, D. Alonso, J. Bond, J. Dumesic. “Reactive Extraction of Levulinate Esters and Conversion to γ-Valerolactone for Production of Liquid Fuels.” *ChemSusChem*, vol. 4, no. 3, **2011**, pp. 357–361., doi:10.1002/cssc.201000396.

[73] L. Yan, N. Yang, H. Pang, B. Liao. “Production of Levulinic Acid from Bagasse and Paddy Straw by Liquefaction in the Presence of Hydrochloride Acid.” *CLEAN – Soil, Air, Water*, vol. 36, no. 2, **2008**, pp. 158–163., doi:10.1002/clen.200700100.

[74] G. Yang, E. Pidko, E. Hensen. “Mechanism of Brønsted Acid-Catalyzed Conversion of Carbohydrates.” *Journal of Catalysis*, vol. 295, **2012**, pp. 122–132., doi:10.1016/j.jcat.2012.08.002.

[75] C. Chang, P. Cen, X. Ma. “Levulinic Acid Production from Wheat Straw.” *Bioresource Technology*, vol. 98, no. 7, **2007**, pp. 1448–1453., doi:10.1016/j.biortech.2006.03.031.

[76] S.W. Fitzpatrick. “The Biofine Technology: A ‘Bio-Refinery’ Concept Based on Thermochemical Conversion of Cellulosic Biomass.” *ACS Symposium Series Feedstocks for the Future*, **2006**, pp. 271–287., doi:10.1021/bk-2006-0921.ch020.

[77] D. Hayes, S. Fitzpatrick, M. Hayes, J. Ross. “The Biofine Process– Production of Levulinic Acid, Furfural, and Formic Acid from Lignocellulosic Feedstocks.” *Biorefineries-Industrial Processes and Products*, **2008**, pp. 139–164., doi:10.1002/9783527619849.ch7.

[78] A. Mukherjee, M.-J. Dumont, V. Raghavan. “Review: Sustainable Production of Hydroxymethylfurfural and Levulinic Acid: Challenges and Opportunities.” *Biomass and Bioenergy*, vol. 72, **2015**, pp. 143–183., doi:10.1016/j.biombioe.2014.11.007.

[79] A.F. Lee, J. Bennett, J. Manayil, K. Wilson. “Heterogeneous Catalysis for Sustainable Biodiesel Production via Esterification and Transesterification.” *Chem. Soc. Rev.*, vol. 43, no. 22, **2014**, pp. 7887–7916., doi:10.1039/c4cs00189c.

[80] S. De, S. Dutta, B. Saha. “Critical Design of Heterogeneous Catalysts for Biomass Valorization: Current Thrust and Emerging Prospects.” *Catalysis Science & Technology*, vol. 6, no. 20, **2016**, pp. 7364–7385., doi:10.1039/c6cy01370h.

[81] M.T. Reche, A. Osatiashtiani, L.J. Durndell, M.A. Isaacs, Â. Silva, A.F. Lee, K. Wilson. “Niobic Acid Nanoparticle Catalysts for the Aqueous Phase Transformation of Glucose and Fructose to 5-Hydroxymethylfurfural.” *Catalysis Science & Technology*, vol. 6, no. 19, **2016**, pp. 7334–7341., doi:10.1039/c6cy01129b.

[82] K. Nakajima, Y. Baba, R. Noma, M. Kitano, J.N. Kondo, S. Hayashi, M. Hara. “Nb2O5·nH2O As a Heterogeneous Catalyst with Water-Tolerant Lewis Acid Sites.” *Journal of the American Chemical Society*, vol. 133, no. 12, **2011**, pp. 4224–4227., doi:10.1021/ja110482r.

[83] R. Noma, K. Nakajima, K. Kamata, M. Kitano, S. Hayashi, M. Hara. “Formation of 5-(Hydroxymethyl)Furfural by Stepwise Dehydration over TiO_2 with Water-Tolerant Lewis Acid Sites.” *The Journal of Physical Chemistry C*, vol. 119, no. 30, **2015**, pp. 17117–17125., doi:10.1021/acs.jpcc.5b03290.

[84] A. Onda, T. Ochi, K. Yanagisawa. “Selective Hydrolysis of Cellulose into Glucose over Solid Acid Catalysts.” *Green Chemistry*, vol. 10, no. 10, **2008**, p. 1033., doi:10.1039/b808471h.

[85] K. Ishida, S. Matsuda, M. Watanabe, H. Kitajima, A. Kato, M. Iguchi, T.M. Aida, R.L. Smith Jr, X. Qi, T. Tago, T. Masuda. “Hydrolysis of Cellulose to Produce Glucose with Solid Acid Catalysts in 1-Butyl-3-Methyl-Imidazolium Chloride ([BmIm][Cl]) with Sequential Water Addition.” *Biomass Conversion and Biorefinery*, vol. 4, no. 4, **2014**, pp. 323–331., doi:10.1007/s13399-014-0116-8.

[86] P.F. Siril, H.E. Cross, D.R. Brown. “New Polystyrene Sulfonic Acid Resin Catalysts with Enhanced Acidic and Catalytic Properties.” *Journal of Molecular Catalysis A: Chemical*, vol. 279, no. 1, **2008**, pp. 63–68., doi:10.1016/j.molcata.2007.10.001.

[87] H. Li, S. Yang, S. Saravanamurugan, A. Riisager. “Glucose Isomerization by Enzymes and Chemo-Catalysts: Status and Current Advances.” *ACS Catalysis*, vol. 7, no. 4, **2017**, pp. 3010–3029., doi:10.1021/acscatal.6b03625.

[88] R. Otomo, T. Yokoi, J.N. Kondo, T. Tatsumi. “Dealuminated Beta Zeolite as Effective Bifunctional Catalyst for Direct Transformation of Glucose to 5-Hydroxymethylfurfural.” *Applied Catalysis A: General*, vol. 470, **2014**, pp. 318–326., doi:10.1016/j.apcata.2013.11.012.

[89] N.M. Xavier, S.D. Lucas, A.P. Rauter. Xavier, Nuno M. “ChemInform Abstract: Zeolites as Efficient Catalysts for Key Transformations in Carbohydrate Chemistry.” *ChemInform*, vol. 40, no. 50, **2009**, doi:10.1002/chin.200950257.

[90] B.F.M. Kuster. “5-Hydroxymethylfurfural (HMF). A Review Focussing on Its Manufacture.” *Starch - Stärke*, vol. 42, no. 8, **1990**, pp. 314–321., doi:10.1002/star.19900420808.

[91] N.A.S. Ramli, N.A.S. Amin. “Fe/HY Zeolite as an Effective Catalyst for Levulinic Acid Production from Glucose: Characterization and Catalytic Performance.” *Applied Catalysis B: Environmental*, vol. 163, **2015**, pp. 487–498., doi:10.1016/j.apcatb.2014.08.031.

[92] J. Jae, G.A. Tompsett, A.J. Foster, K.D. Hammond, S.M. Auerbach, R.F. Lobo, G.W. Huber. “Investigation into the Shape Selectivity of Zeolite Catalysts for Biomass Conversion.” *Journal of Catalysis*, vol. 279, no. 2, **2011**, pp. 257–268., doi:10.1016/j.jcat.2011.01.019.

[93] R. O'Neill, M.N. Ahmad, L. Vanoye, F. Aiouache. "Kinetics of Aqueous Phase Dehydration of Xylose into Furfural Catalyzed by ZSM-5 Zeolite." *Industrial & Engineering Chemistry Research*, vol. 48, no. 9, **2009**, pp. 4300–4306., doi:10.1021/ie801599k.

[94] R. Rinaldi, R. Palkovits, F. Schüth. "Depolymerization of Cellulose Using Solid Catalysts in Ionic Liquids." *Angewandte Chemie International Edition*, vol. 47, no. 42, **2008**, pp. 8047–8050., doi:10.1002/anie.200802879.

[95] M. Käldström, N. Kumar, M. Tenho, M. Mokeev, Y. Moskalenko, D. Murzin. Käldström, Mats. "Catalytic Transformations of Birch Kraft Pulp." *ACS Catalysis*, vol. 2, no. 7, **2012**, pp. 1381–1393., doi:10.1021/cs2006839.

[96] J. Seddon, M. Raimondi. "Liquid Crystal Templating of Mesoporous Materials." *Molecular Crystals and Liquid Crystals Science and Technology. Section A. Molecular Crystals and Liquid Crystals*, vol. 347, no. 1, **2000**, pp. 221–229., doi:10.1080/10587250008024843.

[97] M. Signoretto, A. Breda, F. Somma, F. Pinna, G. Cruciani. "Mesoporous Sulphated Zirconia by Liquid-Crystal Templating Method." *Microporous and Mesoporous Materials*, vol. 91, no. 1-3, **2006**, pp. 23–32., doi:10.1016/j.micromeso.2005.11.004.

[98] T. Yanagisawa, T. Shimizu, K. Kuroda, C. Kato. "The Preparation of Alkyltriinethylaininonium–Kaneinite Complexes and Their Conversion to Microporous Materials." *Bulletin of the Chemical Society of Japan*, vol. 63, no. 4, **1990**, pp. 988–992., doi:10.1246/bcsj.63.988.

[99] J. Beck, J. Vartuli, W. Roth, M. Leonowicz, C. Kresge, K. Schmitt, C. Chu, D. Olson, E. Sheppard, S. Mccullen, J. Higgins, J. Schlenker. "A New Family of Mesoporous Molecular Sieves Prepared with Liquid Crystal Templates." *Journal of the American Chemical Society*, vol. 114, no. 27, **1992**, pp. 10834–10843., doi:10.1021/ja00053a020.

[100] A. Walcarius. "Mesoporous Materials and Electrochemistry." *Chemical Society Reviews*, vol. 42, no. 9, **2013**, p. 4098., doi:10.1039/c2cs35322a.

[101] D. Zhao, J. Feng, Q. Huo, N. Melosh, G.H. Fredrickson, B.F. Chmelka, G.D. Stucky. "Triblock Copolymer Syntheses of Mesoporous Silica with Periodic 50 to 300 Angstrom

Pores." *Science*, vol. 279, no. 5350, **1998**, pp. 548–552., doi:10.1126/science.279.5350.548.

[102] D. Zhao, Q. Huo, J. Feng, B. Chmelka, G. Stucky. "Nonionic Triblock and Star Diblock Copolymer and Oligomeric Surfactant Syntheses of Highly Ordered, Hydrothermally Stable, Mesoporous Silica Structures." *Journal of the American Chemical Society*, vol. 120, no. 24, **1998**, pp. 6024–6036., doi:10.1021/ja974025i.

[103] D. Zhao, J. Sun, Q. Li, G. Stucky. "Morphological Control of Highly Ordered Mesoporous Silica SBA-15." *Chemistry of Materials*, vol. 12, no. 2, **2000**, pp. 275–279., doi:10.1021/cm9911363.

[104] P.T. Tanev, T.J. Pinnavaia. "A Neutral Templating Route to Mesoporous Molecular Sieves." *Science*, vol. 267, no. 5199, **1995**, pp. 865–867., doi:10.1126/science.267.5199.865.

[105] Q. Huo, D.I. Margolese, U. Ciesla, P. Feng, T.E. Gier, P. Sieger, R. Leon, P.M. Petroff, F. Schüth, G.D. Stucky. "Generalized Synthesis of Periodic Surfactant/Inorganic Composite Materials." *Nature*, vol. 368, no. 6469, **1994**, pp. 317–321., doi:10.1038/368317a0.

[106] F. Renzo, D. Desplantier, A. Galarneau, F. Fajula. "Micelle Templating for the Formulation of Silica at the Nanometer Scale." *Catalysis Today*, vol. 66, no. 1, **2001**, pp. 75–79., doi:10.1016/s0920-5861(00)00606-4.

[107] K. Cassiers, T. Linssen, M. Mathieu, M. Benjelloun, K. Schrijnemakers, P. Voort, P. Cool, E.F. Vansant. "A Detailed Study of Thermal, Hydrothermal, and Mechanical Stabilities of a Wide Range of Surfactant Assembled Mesoporous Silicas." *Chemistry of Materials*, vol. 14, no. 5, **2002**, pp. 2317–2324., doi:10.1021/cm0112892.

[108] Z.Y. Wu, H.J. Wang, T.T. Zhuang, L.B. Sun, Y.M. Wang, J.H. Zhu. "Multiple Functionalization of Mesoporous Silica in One-Pot: Direct Synthesis of Aluminum-Containing Plugged SBA-15 from Aqueous Nitrate Solutions." *Advanced Functional Materials*, vol. 18, no. 1, **2008**, pp. 82–94., doi:10.1002/adfm.200700706.

[109] A. Zukal, H. Šiklová, J. Čejka. “Grafting of Alumina on SBA-15: Effect of Surface Roughness.” *Langmuir*, vol. 24, no. 17, **2008**, pp. 9837–9842., doi:10.1021/la801547u.

[110] M. Zakharova, F. Kleitz, F.-G. Fontaine. “Lewis Acidity Quantification and Catalytic Activity of Ti, Zr and Al-Supported Mesoporous Silica.” *Dalton Transactions*, vol. 46, no. 12, **2017**, pp. 3864–3876., doi:10.1039/c7dt00035a.

[111] Â. Silva, K. Wilson, A. Lee, V. Santos, A. Bacilla, K. Mantovani, S. Nakagaki. “Nb_2O_5 /SBA-15 Catalyzed Propanoic Acid Esterification.” *Applied Catalysis B: Environmental*, vol. 205, **2017**, pp. 498–504., doi:10.1016/j.apcatb.2016.12.066.

[112] Y. Li, W. Zhang, L. Zhang, Q. Yang, Z. Wei, Z. Feng, C. Li. “Direct Synthesis of Al−SBA-15 Mesoporous Materials via Hydrolysis-Controlled Approach.” *The Journal of Physical Chemistry B*, vol. 108, no. 28, **2004**, pp. 9739–9744., doi:10.1021/jp049824j.

[113] P. Bhange, D. Bhange, S. Pradhan, V. Ramaswamy. “Direct Synthesis of Well-Ordered Mesoporous Al-SBA-15 and Its Correlation with the Catalytic Activity.” *Applied Catalysis A: General*, vol. 400, no. 1-2, **2011**, pp. 176–184., doi:10.1016/j.apcata.2011.04.031.

[114] Y. Kim, G. Shao, S. Jeon, S.M. Imran, P. Sarawade, H. Kim. “Sol–Gel Synthesis of Sodium Silicate and Titanium Oxychloride Based TiO_2–SiO_2 Aerogels and Their Photocatalytic Property under UV Irradiation.” *Chemical Engineering Journal*, vol. 231, **2013**, pp. 502–511., doi:10.1016/j.cej.2013.07.072.

[115] K.-S. Cho, Y.-K. Lee. “Effects of Nitrogen Compounds, Aromatics, and Aprotic Solvents on the Oxidative Desulfurization (ODS) of Light Cycle Oil over Ti-SBA-15 Catalyst.” *Applied Catalysis B: Environmental*, vol. 147, **2014**, pp. 35–42., doi:10.1016/j.apcatb.2013.08.017.

[116] D. Georgescu, A.-M. Brezoiu, R.-A. Mitran, D. Berger, C. Matei, B. Negreanu-Pirjol. “Mesostructured Silica–Titania Composites for Improved Oxytetracycline Delivery Systems.” *Comptes Rendus Chimie*, vol. 20, no. 11-12, **2017**, pp. 1017–1025., doi:10.1016/j.crci.2017.09.006.

[117] J. Dhainaut, J.-P. Dacquin, A. Lee, K. Wilson. “Hierarchical Macroporous–Mesoporous SBA-15 Sulfonic Acidcatalysts for Biodiesel Synthesis.” *Green Chem.*, vol. 12, no. 2, **2010**, pp. 296–303., doi:10.1039/b919341c.

[118] C. Pirez, J.-M. Caderon, J.-P. Dacquin, A. Lee, K. Wilson. “Tunable KIT-6 Mesoporous Sulfonic Acid Catalysts for Fatty Acid Esterification.” *ACS Catalysis*, vol. 2, no. 8, **2012**, pp. 1607–1614., doi:10.1021/cs300161a.

[119] S. Li, E. Qian, T. Shibata, M. Hosomi. “Catalytic Hydrothermal Saccharification of Rice Straw Using Mesoporous Silica-Based Solid Acid Catalysts.” *Journal of the Japan Petroleum Institute*, vol. 55, no. 4, **2012**, pp. 250–260., doi:10.1627/jpi.55.250.

[120] C. Pirez, A. Lee, J. Manayil, C. Parlett, K. Wilson. “Hydrothermal Saline Promoted Grafting: a Route to Sulfonic Acid SBA-15 Silica with Ultra-High Acid Site Loading for Biodiesel Synthesis.” *Green Chem.*, vol. 16, no. 10, **2014**, pp. 4506–4509., doi:10.1039/c4gc01139b.

[121] S.-Y. Chen, T. Mochizuki, Y. Abe, M. Toba, Y. Yoshimura. “Production of High-Quality Biodiesel Fuels from Various Vegetable Oils over Ti-Incorporated SBA-15 Mesoporous Silica.” *Catalysis Communications*, vol. 41, **2013**, pp. 136–139., doi:10.1016/j.catcom.2013.07.021.

[122] X. Feng, G. Fryxell, L.-Q. Wang, A. Kim, J. Liu, K. Kemner. “Functionalized Monolayers on Ordered Mesoporous Supports.” *Science*, vol. 276, no. 5314, **1997**, pp. 923–926., doi:10.1126/science.276.5314.923.

[123] J.P. Dacquin, A.F. Lee, C. Pirez, K. Wilson. “Pore-Expanded SBA-15 Sulfonic Acid Silicas for Biodiesel Synthesis.” *Chem. Commun.*, vol. 48, no. 2, **2012**, pp. 212–214., doi:10.1039/c1cc14563k.

[124] D.H. Everett. “Thermodynamics of Interfacial Phenomena.” *Pure and Applied Chemistry*, vol. 53, no. 11, **1981**, pp. 2181–2198., doi:10.1351/pac198153112181.

[125] X.S. Zhao, G.Q. Lu, G.J. Millar. “Advances in Mesoporous Molecular Sieve MCM-41.” *Industrial & Engineering Chemistry Research*, vol. 35, no. 7, **1996**, pp. 2075–2090., doi:10.1021/ie950702a.

[126] G. Leofanti, M. Padovan, G. Tozzola, B. Venturelli. “Surface Area and Pore Texture of Catalysts.” *Catalysis Today*, vol. 41, no. 1-3, **1998**, pp. 207–219., doi:10.1016/s0920-5861(98)00050-9.

[127] Z.A. Alothman. “A Review: Fundamental Aspects of Silicate Mesoporous Materials.” *Materials*, vol. 5, no. 12, **2012**, pp. 2874–2902., doi:10.3390/ma5122874.

[128] I.L. Mostinsky. “Adsorption.” *A-To-Z Guide to Thermodynamics, Heat and Mass Transfer, and Fluids Engineering*, doi:10.1615/atoz.a.adsorption.

[129] Y. Waseda, E. Matsubara, K. Shinoda. “X-Ray Diffraction Crystallography.” **2011**, doi:10.1007/978-3-642-16635-8.

[130] J. W. Niemantsverdriet. “Spectroscopy in Catalysis.” **2007**, doi:10.1002/9783527611348.

[131] V. Trevisan, A. Olivo, F. Pinna, M. Signoretto, F. Vindigni, G. Cerrato, C.l. Bianchi. “C-N/TiO_2 Photocatalysts: Effect of Co-Doping on the Catalytic Performance under Visible Light.” *Applied Catalysis B: Environmental*, vol. 160-161, **2014**, pp. 152–160., doi:10.1016/j.apcatb.2014.05.015.

[132] M.J. Climent, A. Corma, S. Iborra, S. Martínez-Silvestre. “Transformation of Cellulose into Nonionic Surfactants Using a One-Pot Catalytic Process.” *ChemSusChem*, vol. 9, no. 24, **2016**, pp. 3492–3502., doi:10.1002/cssc.201600977.

[133] S.-Y. Chen, C.-Y. Tang, J.-F. Lee, L.-Y. Jang, T. Tatsumi, S. Cheng. “Effect of Calcination on the Structure and Catalytic Activities of Titanium Incorporated SBA-15.” *J. Mater. Chem.*, vol. 21, no. 7, **2011**, pp. 2255–2265., doi:10.1039/c0jm03111a.

[134] J. Aguado, J.M. Arsuaga, A. Arencibia. “Influence of Synthesis Conditions on Mercury Adsorption Capacity of Propylthiol Functionalized SBA-15 Obtained by Co-Condensation.”

Microporous and Mesoporous Materials, vol. 109, no. 1-3, **2008**, pp. 513–524., doi:10.1016/j.micromeso.2007.05.061.

[135] P-J. Chiu, S. Vetrivel, A.S.T. Chiang, H.-M. Kao. “Synthesis and Characterization of Cubic Periodic Mesoporous Organosilicas with a High Loading of Disulfide Groups.” *New Journal of Chemistry*, vol. 35, no. 2, **2011**, p. 489., doi:10.1039/c0nj00839g.

[136] I.K. Mbaraka, B.H. Shanks. “Acid Strength Variation Due to Spatial Location of Organosulfonic Acid Groups on Mesoporous Silica.” *Journal of Catalysis*, vol. 244, no. 1, **2006**, pp. 78–85., doi:10.1016/j.jcat.2006.09.001.

[137] T. Besson, C.O. Kappe. “Microwave Susceptors.” *Microwaves in Organic Synthesis*, **2013**, pp. 297–346., doi:10.1002/9783527651313.ch7.